universität innsbruck
Institut für Ionenphysik und Angewandte Physik

DK-ALM

Exploring the cosmos: Spectroscopy of Ionic Iron Compounds with Astrochemical Relevance

Basic Principles and Recent Results

GRUND $^{15}{}_{35}$

Shan Jin
Jan. 30th,2025

1. Background

The CCD image of the interstellar medium (ISM), token by Adam Block at the Caelum Observation.

1. Background

Ionized hydrogen

H II regions because of H-α emission

a wavelength of 656.28 nm (red light)

H atom:

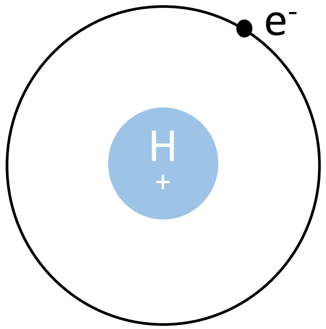

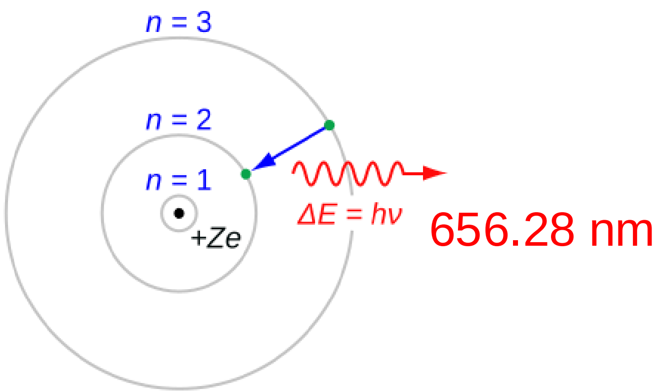

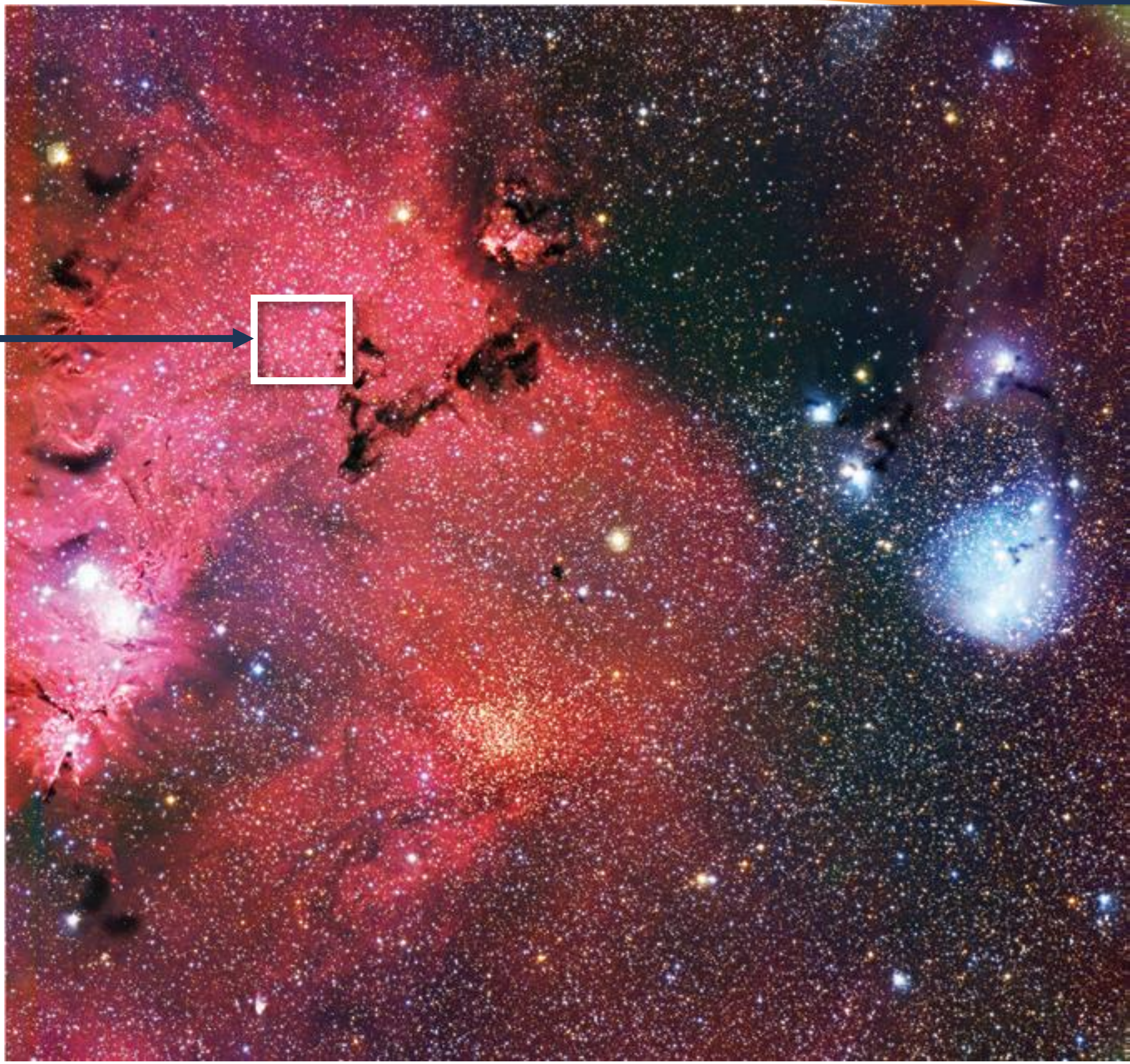

1. Background

Ionized hydrogen
H II regions because of H-α emission

reflection nebulae

???

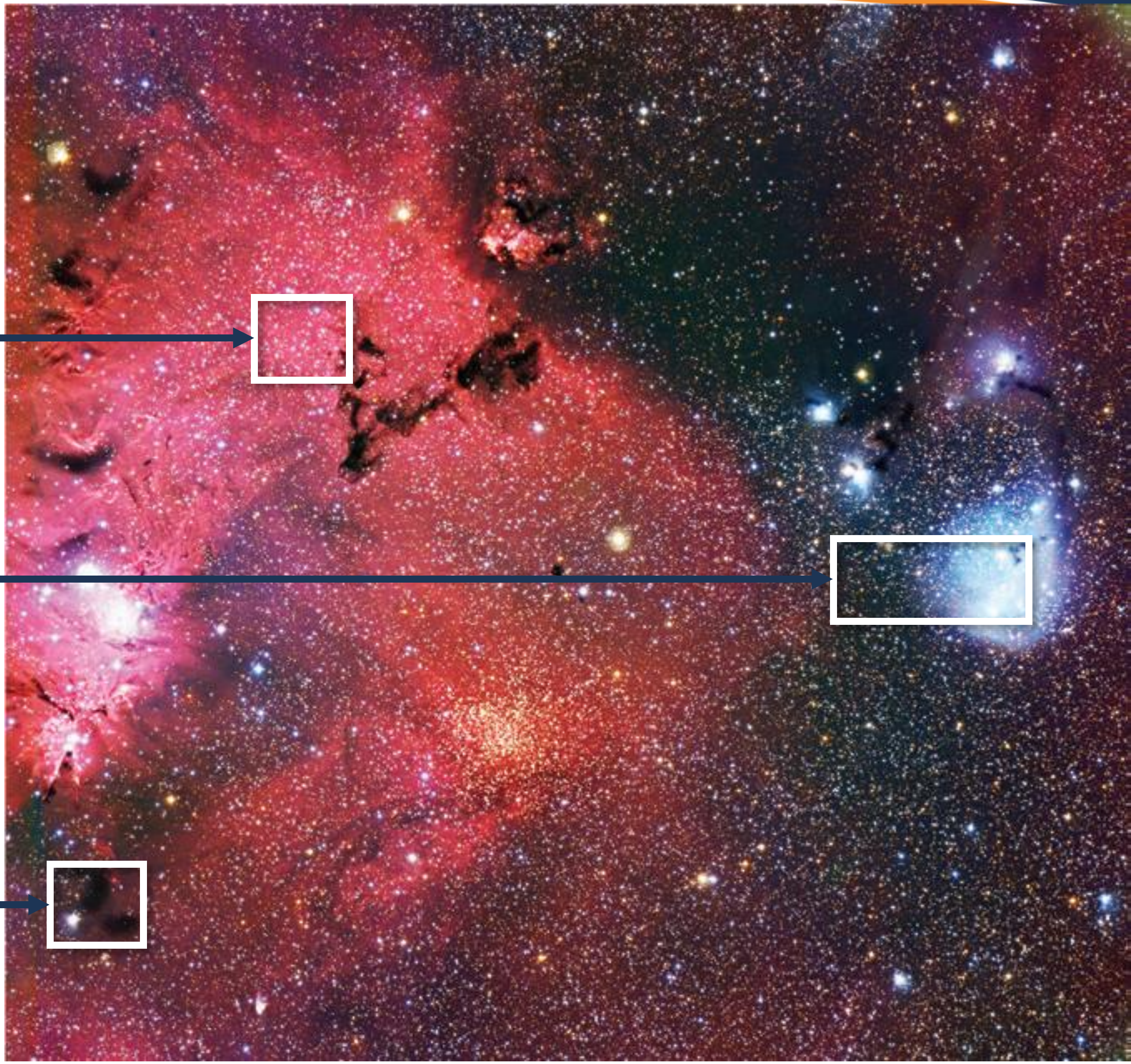

1. Background

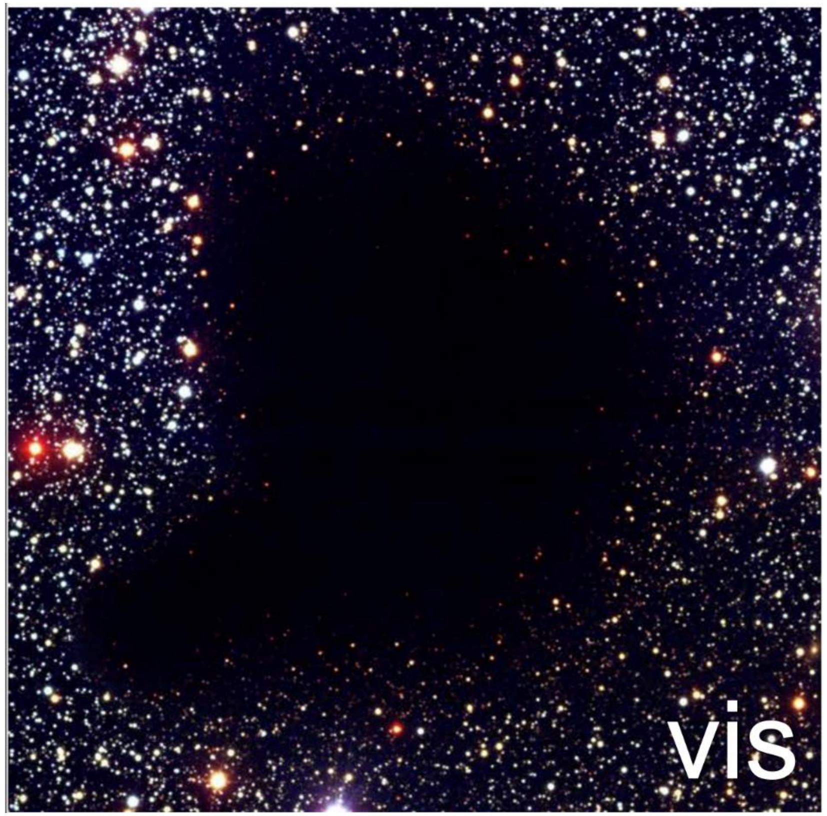

cool dense molecular clouds

[1] Cold molecules, lecture compiled by Prof. Paul Scheier

1. Background

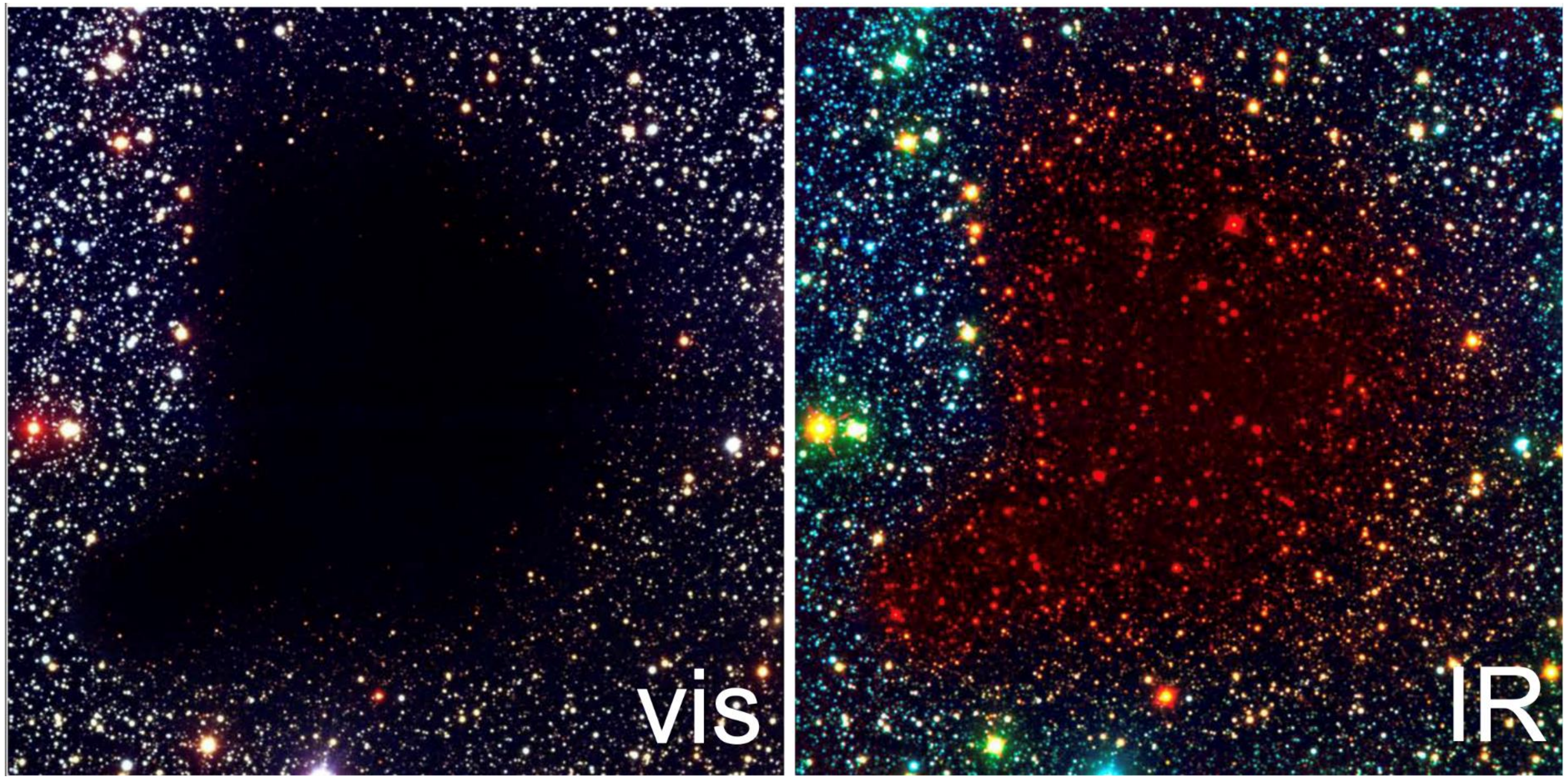

[1] Cold molecules, lecture compiled by Prof. Paul Scheier

1. Background

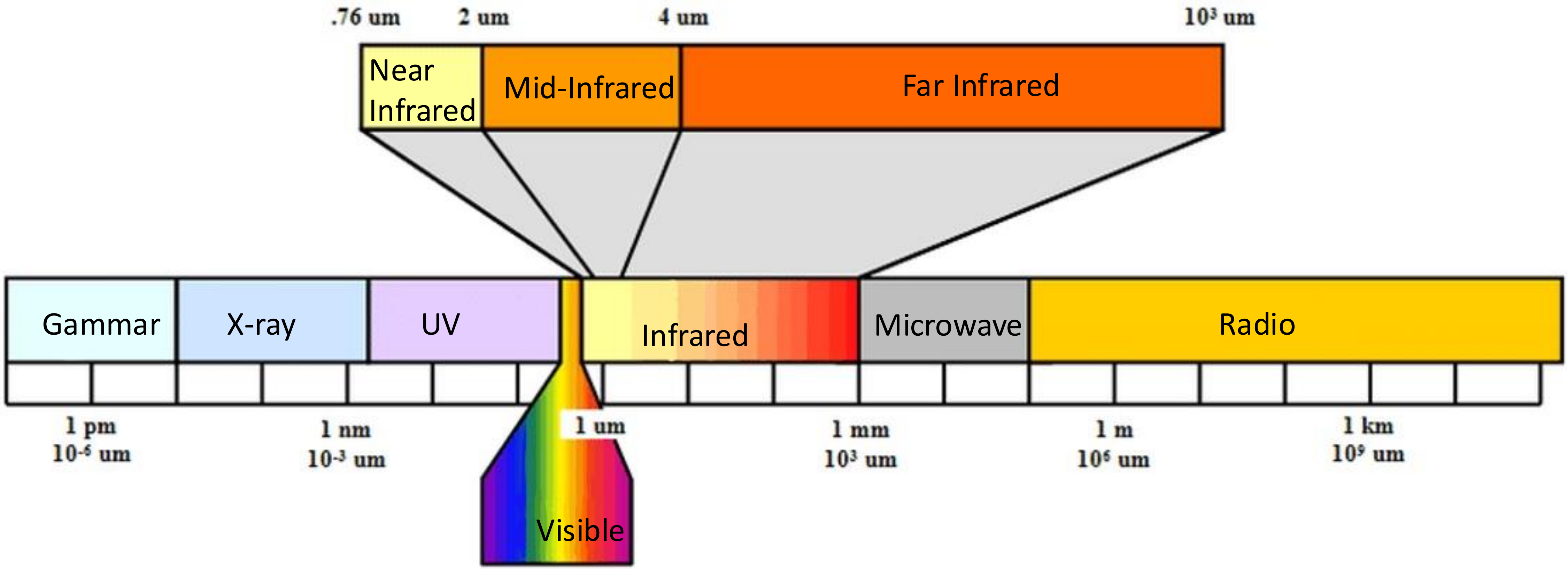

With different telescope covering different region, astrophysicists are able to obtain more information from outerspace.

1. Background

	Temperature / K	Number de… *cm*$^{-3}$
Diffuse clouds	~100	100
Dense clouds	10-100	10^4 -10^8
Accretion disk	10-1000	10^8 -10^{13}



Material	Number density, *n* / *cm*
Ideal gas	2.504 * 10^{19}
Low Earth orbit (300km)	~10^8
Surface of moon	~10^2

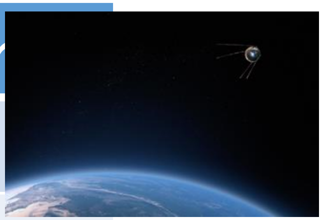


[1] Cold molecules, lecture compiled by Prof. Paul Scheier. [2] Mateo-Marti et al., Life 2019, 9(3), 72.
[3] R.J. Reid, Vacuum science and technology in accelerators, Cockcroft Institute Lectures, 2010.

1. Background

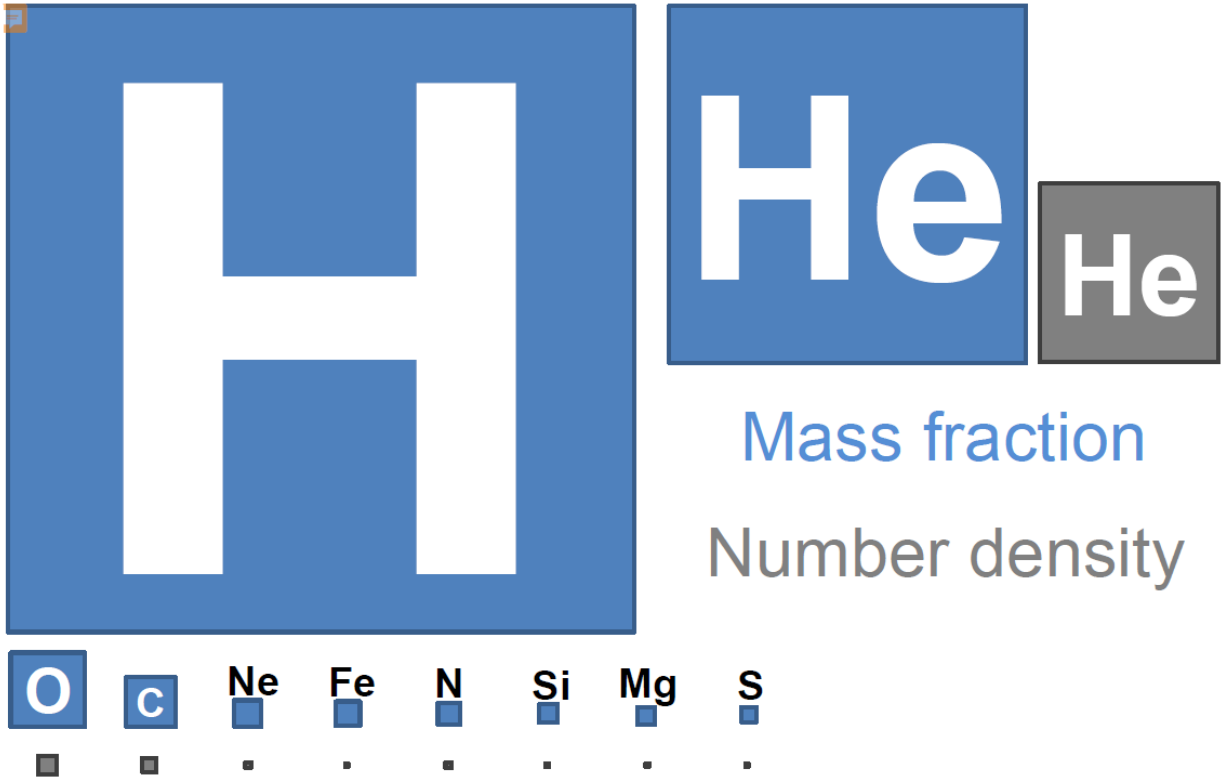

1. Background

Periodic table of astronomers

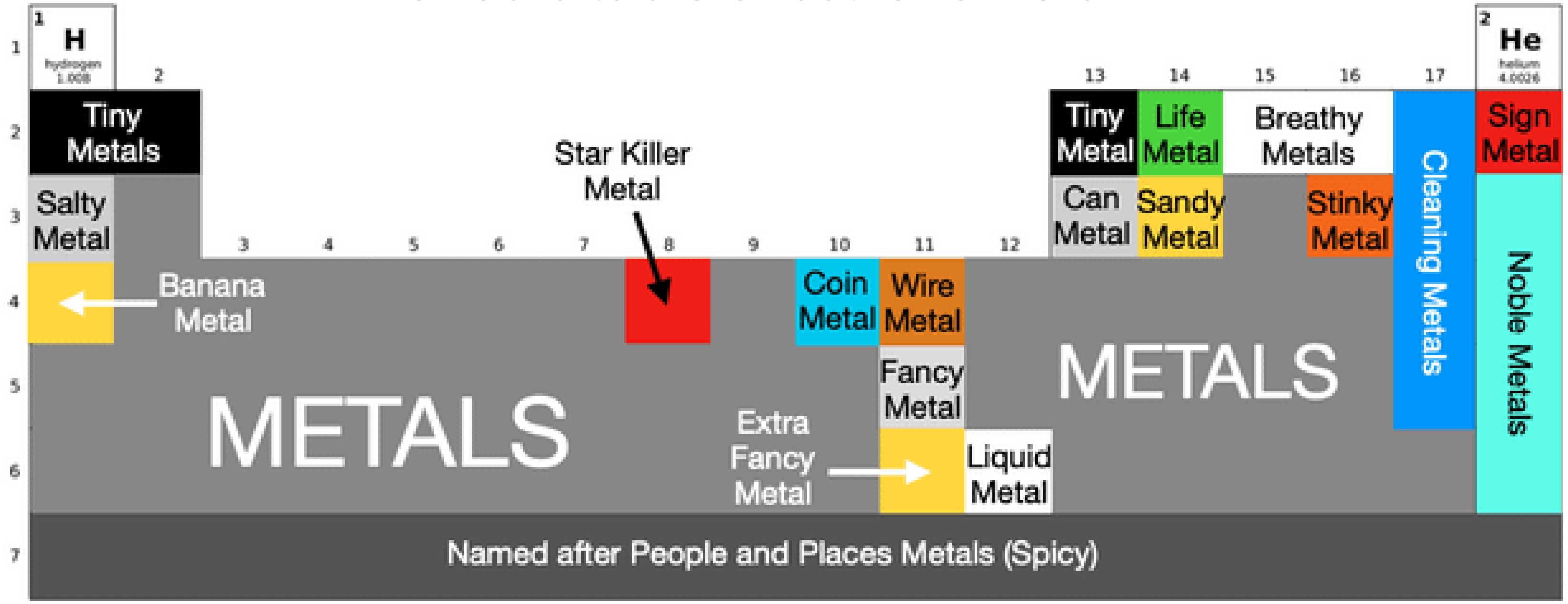

Quiz:

What is the life metal?

What is the star killer metal?

1. Background

Diffuse interstellar medium

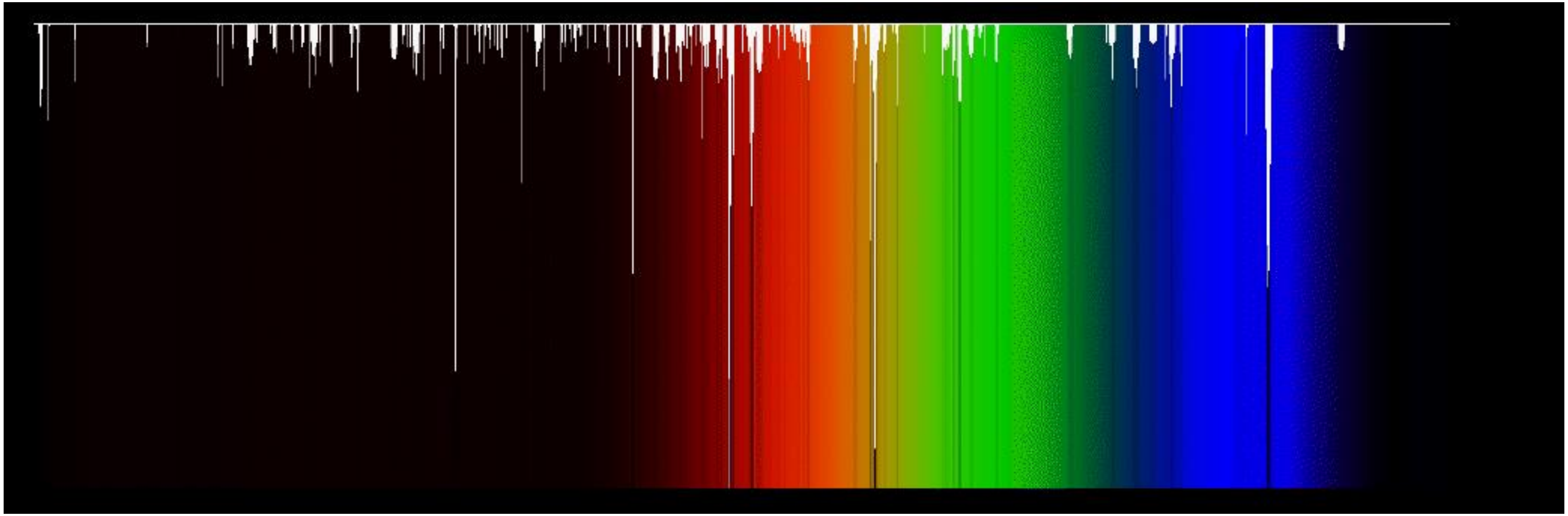

1. Background

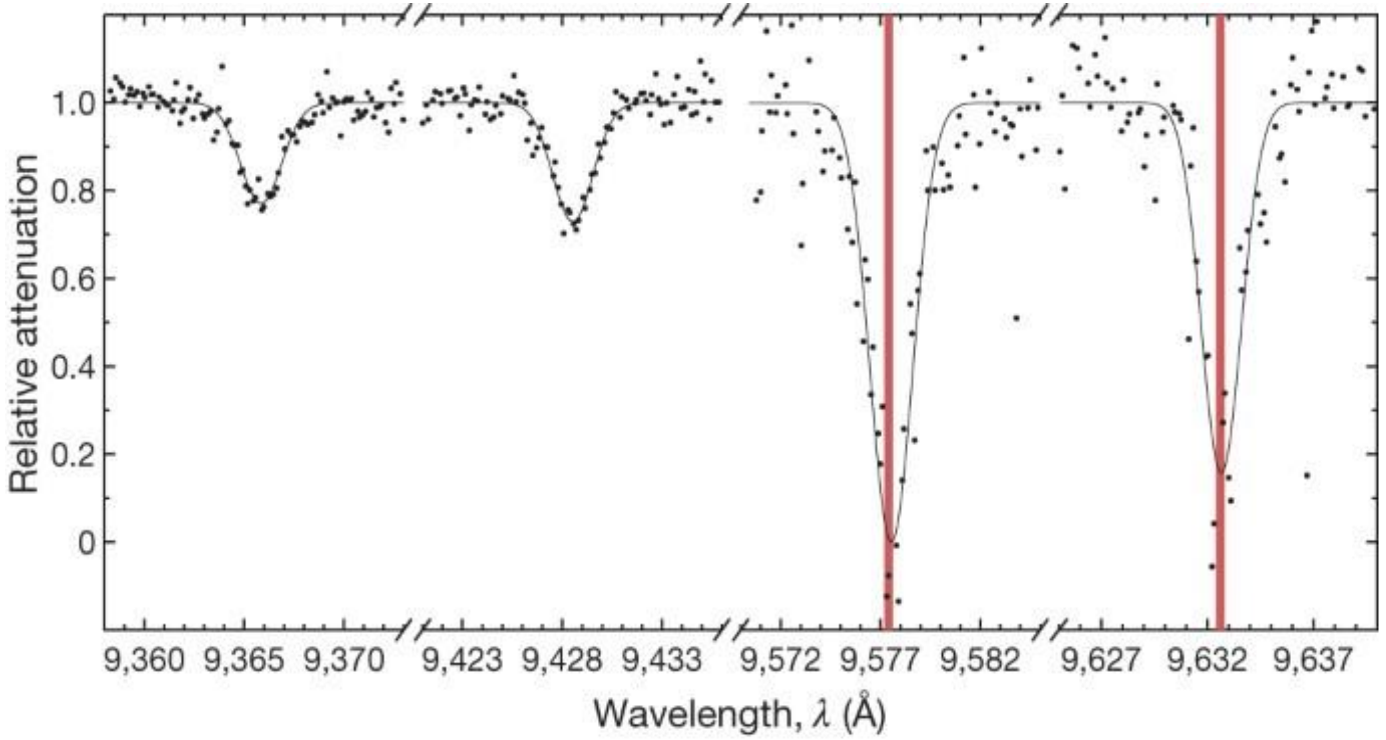

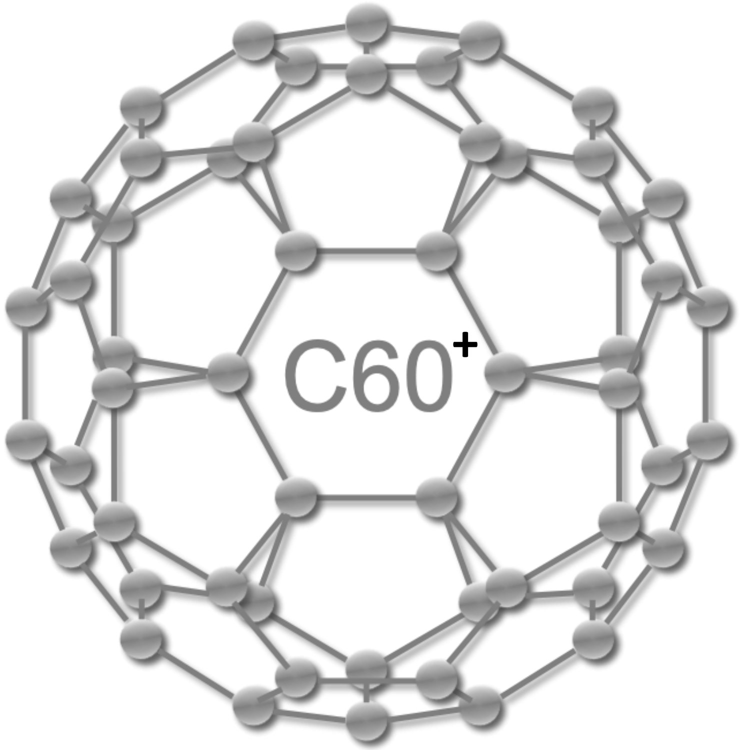

Fe^{+} in the Interstellar Medium

- **Fe** is by far one of the most abundant metals in the universe
- Little atomic iron is seen
- Detection of **FeO** [1] and **FeCN**[2] in the interstellar clouds
- Ion **spectroscopy** + mass **spectrometry** as a high-resolution tool

FeH^{+}

> The FeH^{+} molecule is predicted to be quite abundant based on calculated molecular dissociative equilibria in cool stellar atmospheres, such as those occurring in red giant stars (Johnson & Sauval 1982). It is, therefore, important to under-

[3] S.R. Langhoff, C.W. Bauschlicher Jr., *Astrophysics Journal*, **1991**, 375: 843-845.

[1] The Astrophysical Journal, 566:L109–L112, 2002.
[2] The Astrophysical Journal Letters, 733:L36 (5pp), 2011

Theoretical Methods

Molecules are observed spectroscopically.

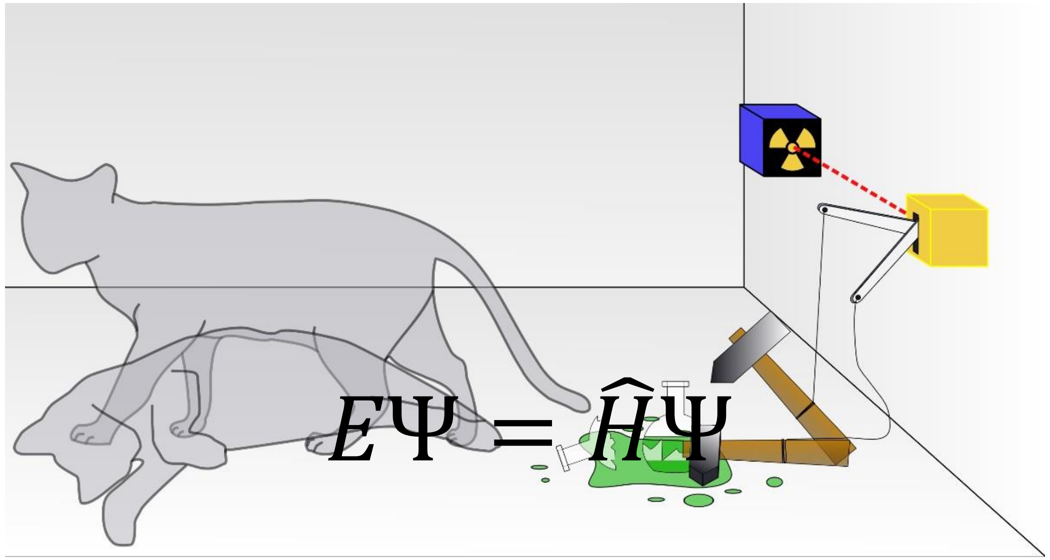

$$E\Psi = \hat{H}\Psi$$

$$\hat{H} = \hat{T}_N + \hat{T}_e + \hat{V}_{eN} + \hat{V}_{ee} + \hat{V}_{NN} \quad \text{------------------ (1)}$$

$$\hat{H}_e = \hat{T}_e + \hat{V}_{eN} + \hat{V}_{NN} \quad \text{------------------ (2)}$$

$\hat{T}_e + \hat{V}_{eN} + \hat{V}_{NN}$ = Hamiltonian for electron motion

$\hat{V}_{NN}$ = Hamiltonian for nu-nu repulsion

Molecules are observed spectroscopically

$$E = E_{el} + E_{vib} + E_{rot}$$

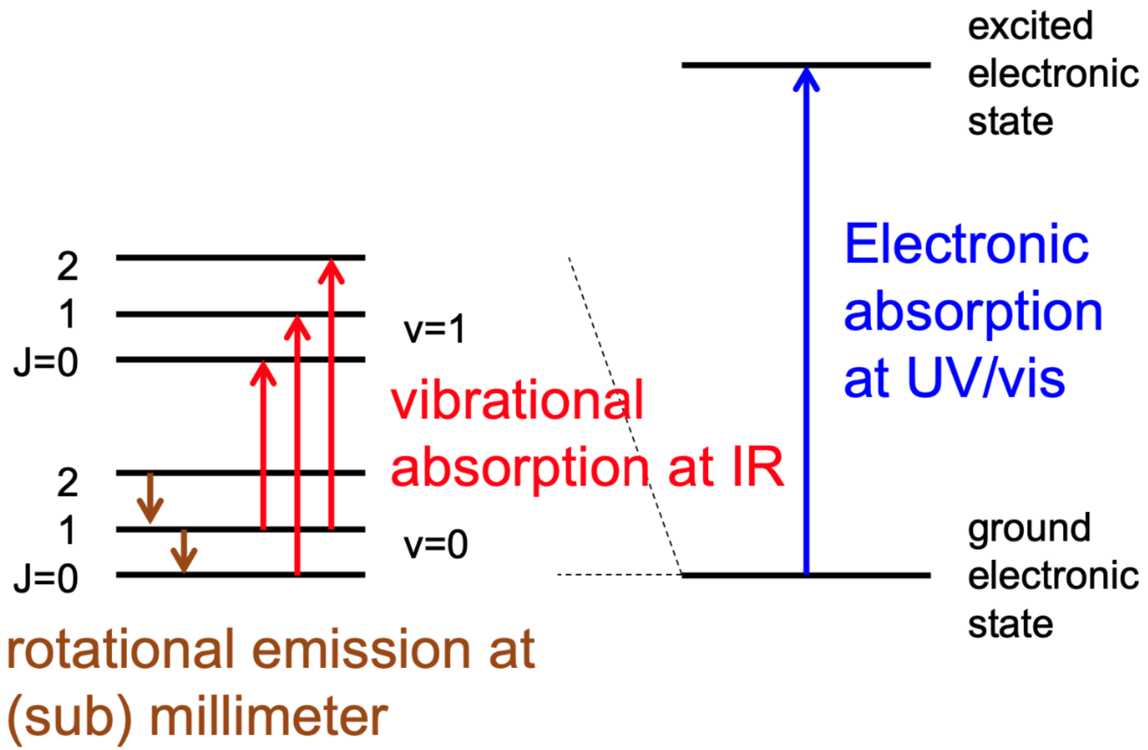

Molecules are observed spectroscopically

Jablonski Diagram

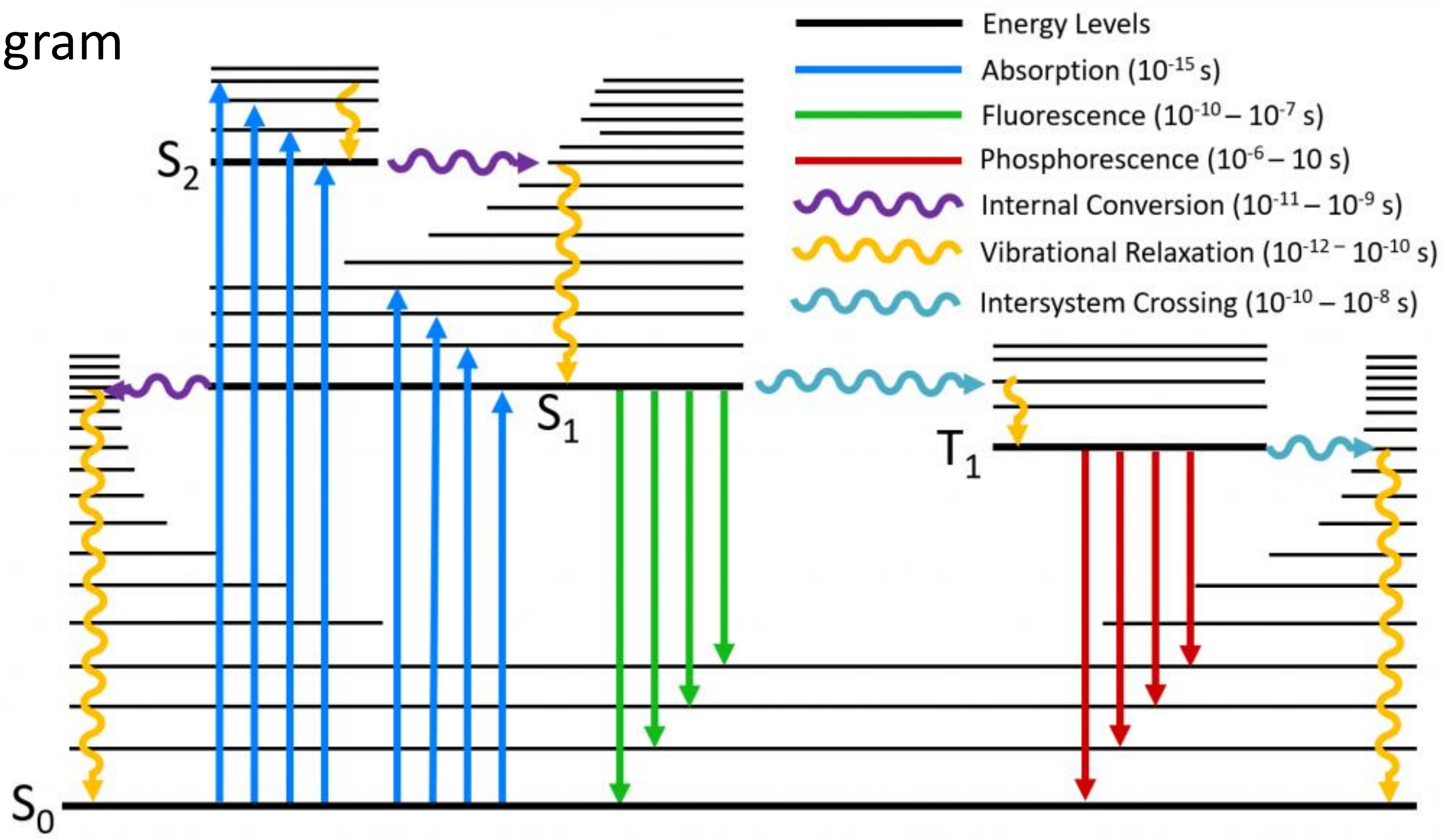

Molecules are observed spectroscopically

$$E = E_{el} + E_{vib} + E_{rot}$$

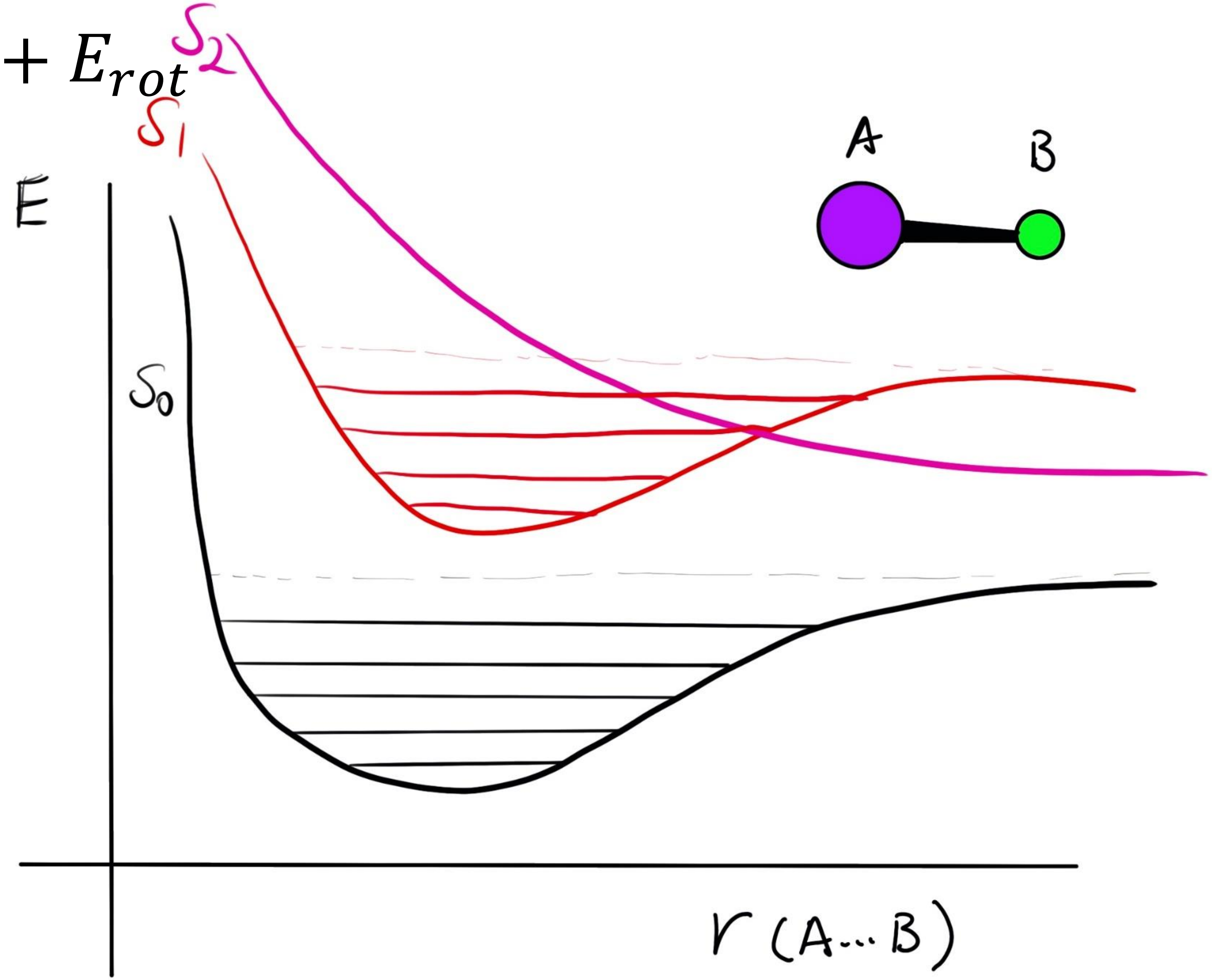

Infrared Multiphoton Dissociation Spectroscopy

Dissociation threshold

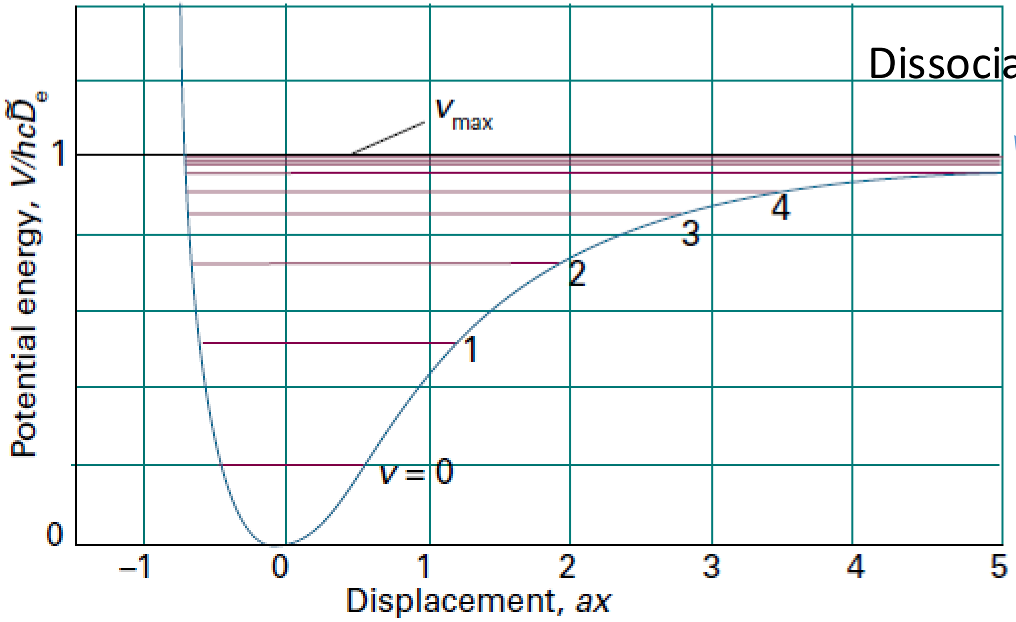

Figure 11C.4 The Morse potential energy curve reproduces the general shape of a molecular potential energy curve. The corresponding Schrödinger equation can be solved, and the values of the energies obtained. The number of bound levels is finite.

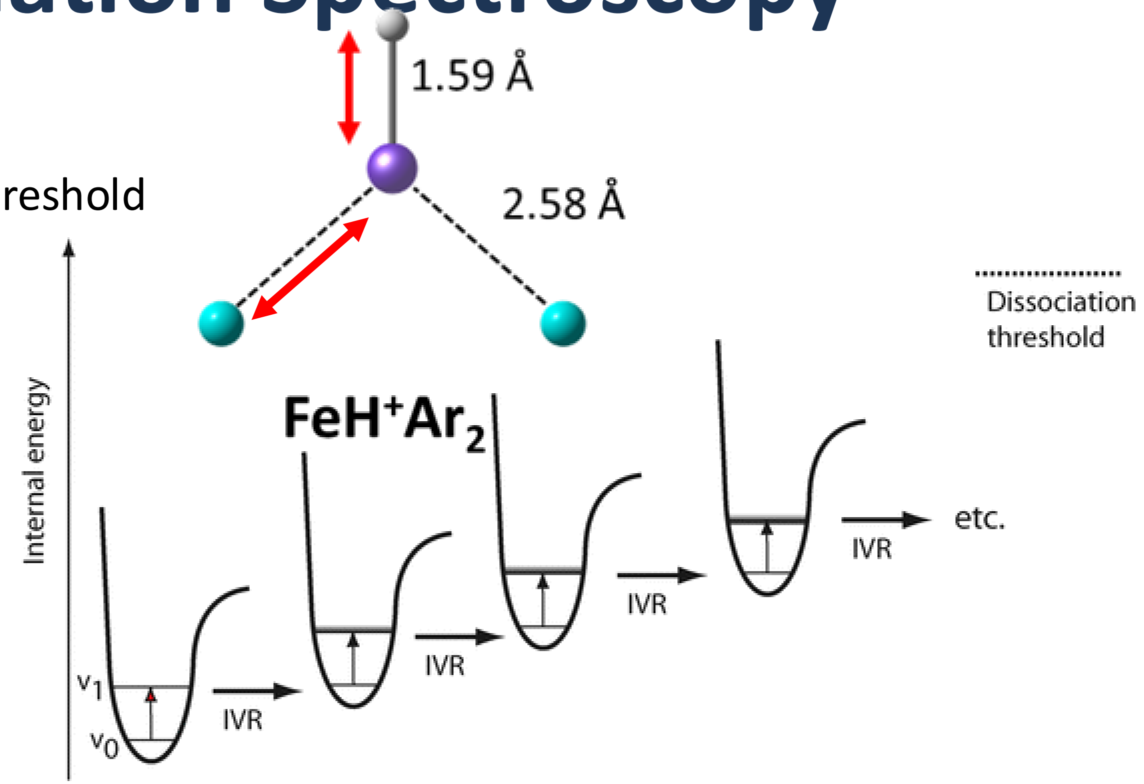

IVR: intramolecular vibrational redistribution

Fundamental, Overtone, Combination band, Hot band, and Isotope effect

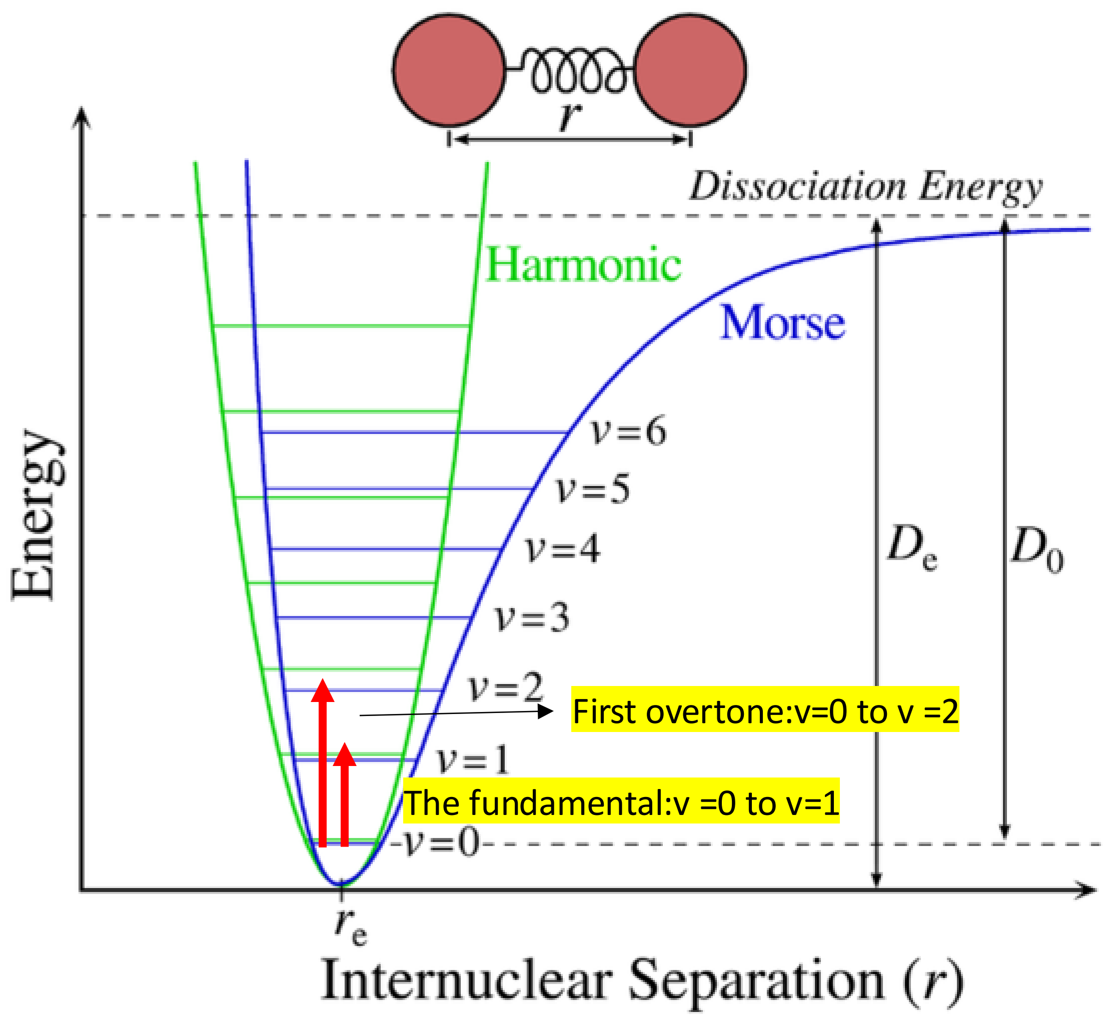

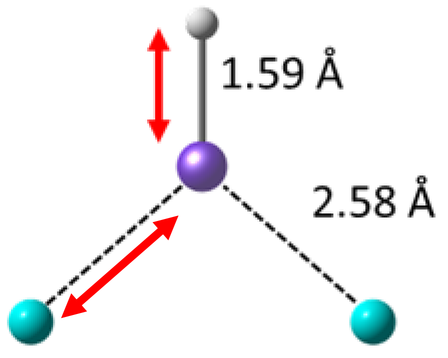

FeH^+Ar_2

Vibrational energy levels

$$\nu_e = \frac{1}{2\pi}\sqrt{\frac{k}{\mu}}$$

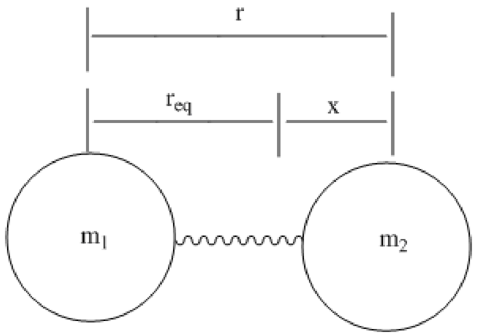

K is the force constant

μ is a reduced mass → $\mu = \frac{m_1 m_2}{m_1 + m_2}$

EXPERIMENTAL SETUP

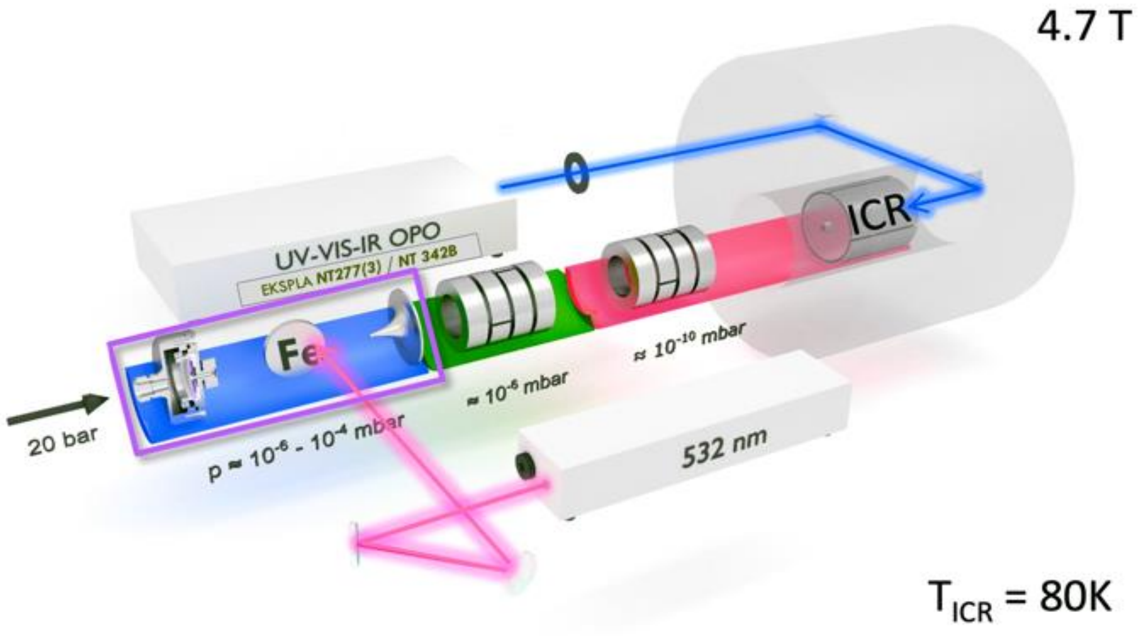

Fourier-Transform Ion Cyclotron Resonance Mass Spectrometry

4.7T FT-ICR @ University of Innsbruck

EXPERIMENTAL SETUP - Vacuum

Vacuum classification

Low vacuum	Atmospheric pressure to 1 mbar
Medium vacuum	1 to 10^{-3} mbar
High vacuum (HV)	10^{-3} to 10^{-8} mbar
Ultrahigh vacuum (UHV)	10^{-8} to 10^{-12} mbar
Extreme high vacuum (XHV)	Less than 10^{-12} mbar

Particle density:

10^{-12} mbar ~$2.5*10^4$

1 bar = 100000 Pa
1 standard atmosphere
= 101325 Pa = 760Torr

EXPERIMENTAL SETUP - Vacuum

Vacuum classification

Low vacuum	Atmospheric pressure to 1 mbar
Medium vacuum	1 to 10^{-3} mbar
High vacuum (HV)	10^{-3} to 10^{-8} mbar
Ultrahigh vacuum (UHV)	10^{-8} to 10^{-12} mbar
Extreme high vacuum (XHV)	Less than 10^{-12} mbar

Particle density:

10^{-12} mbar ~$2.5*10^4$

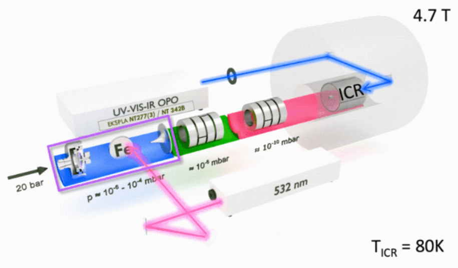

Fourier-Transform Ion Cyclotron Resonance Mass Spectrometry

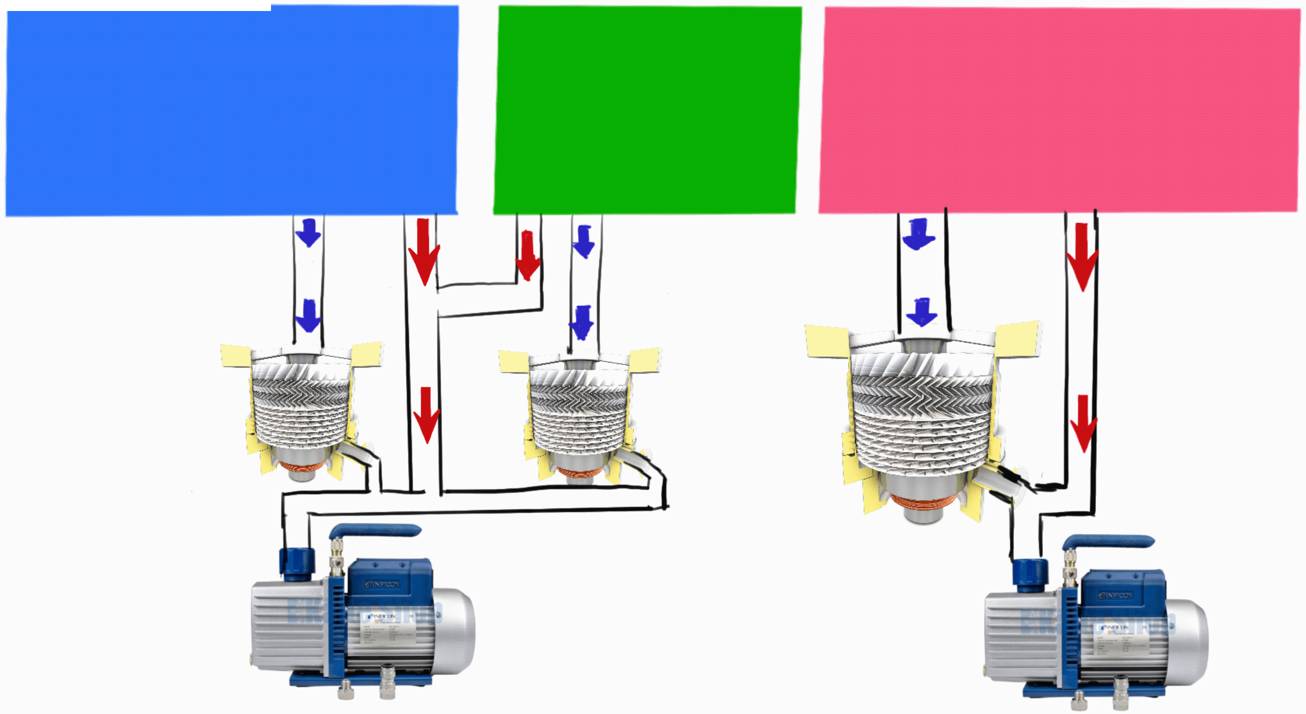

1 bar = 100000 Pa
1 standard atmosphere
= 101325 Pa = 760Torr

EXPERIMENTAL SETUP – Laser Vaporization

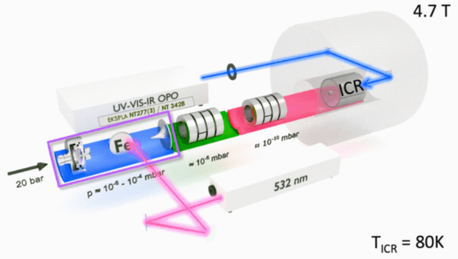

Fourier-Transform Ion Cyclotron Resonance Mass Spectrometry

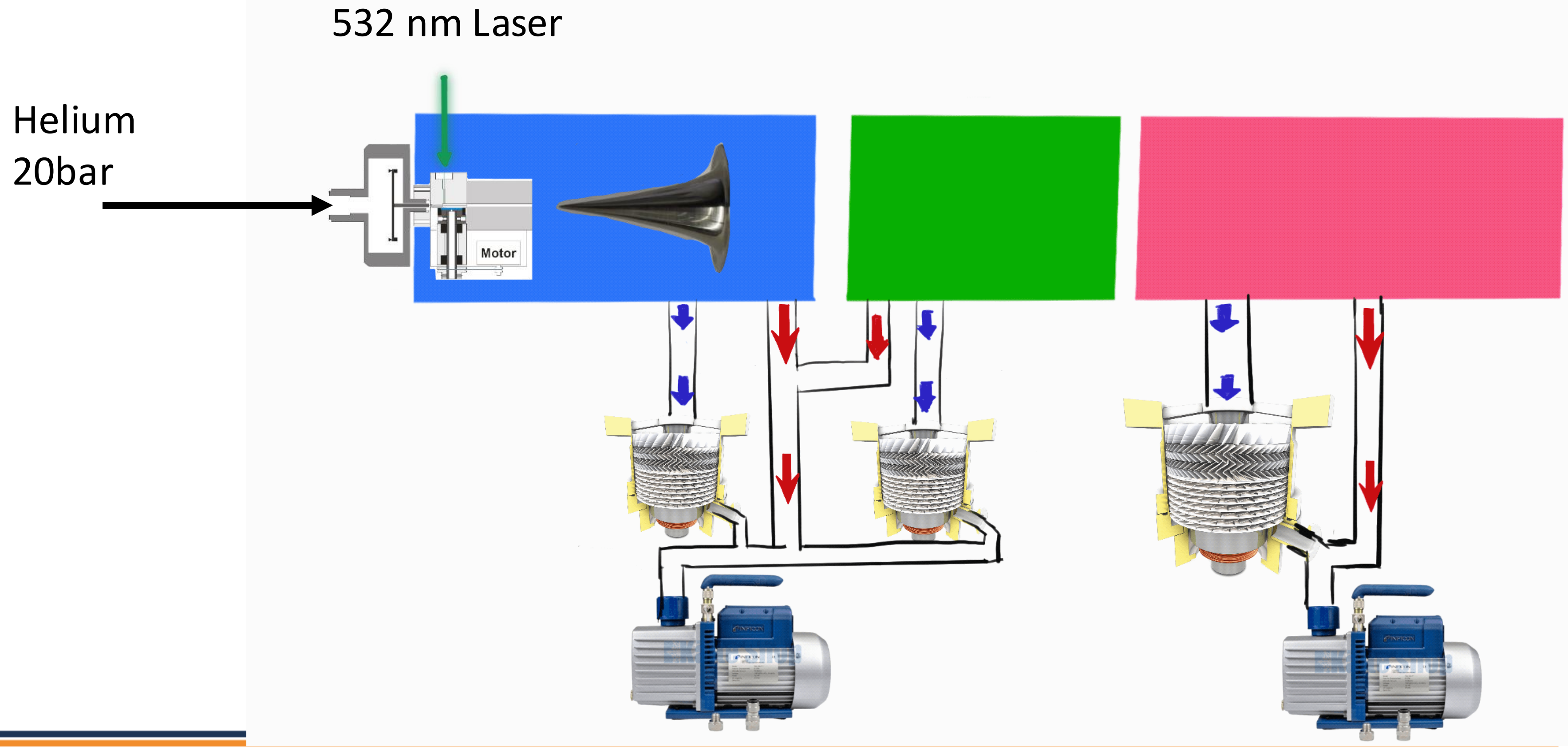

EXPERIMENTAL SETUP - Cooling

Supersonic expansion

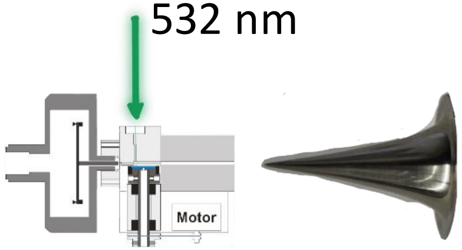

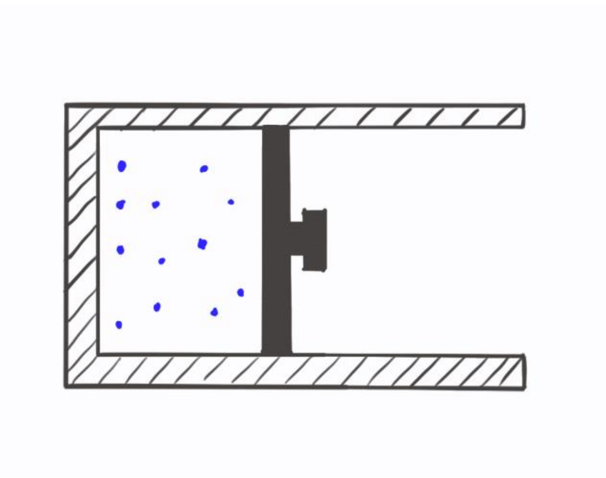

Cryogenic cooling

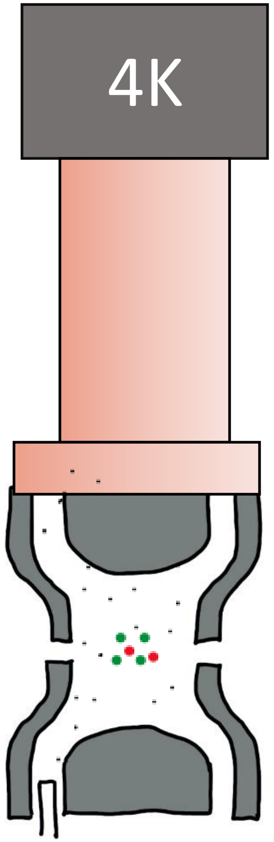

EXPERIMENTAL SETUP– Ion optics

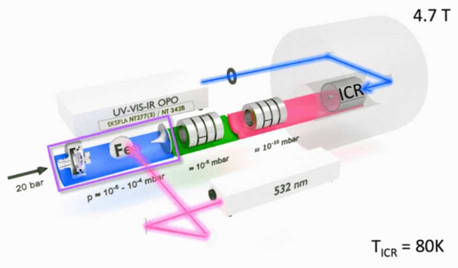

Fourier-Transform Ion Cyclotron Resonance Mass Spectrometry

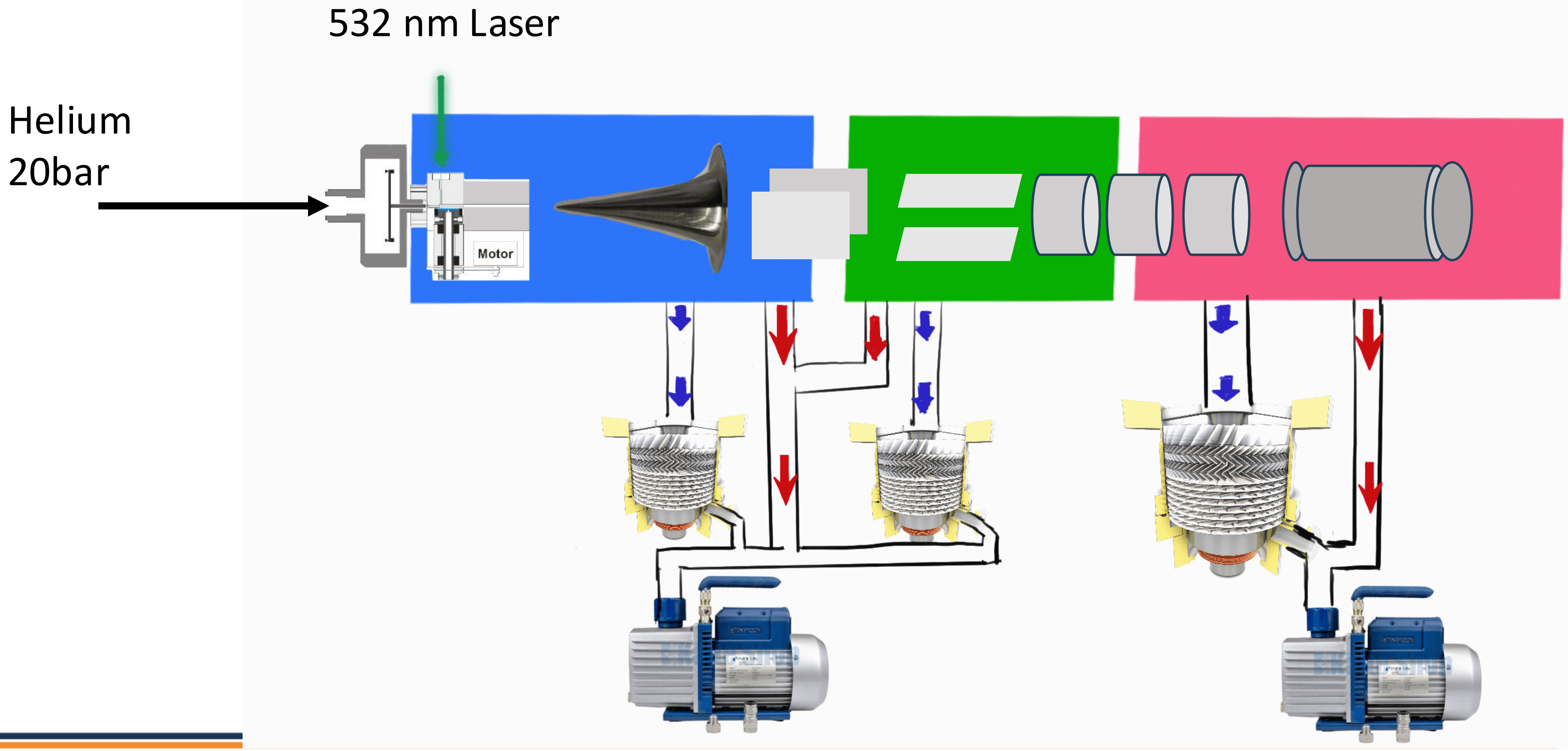

EXPERIMENTA

light

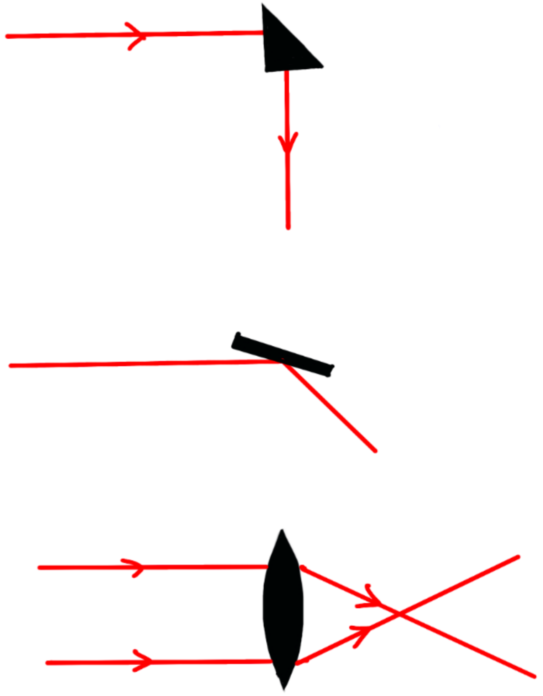

Charged partic

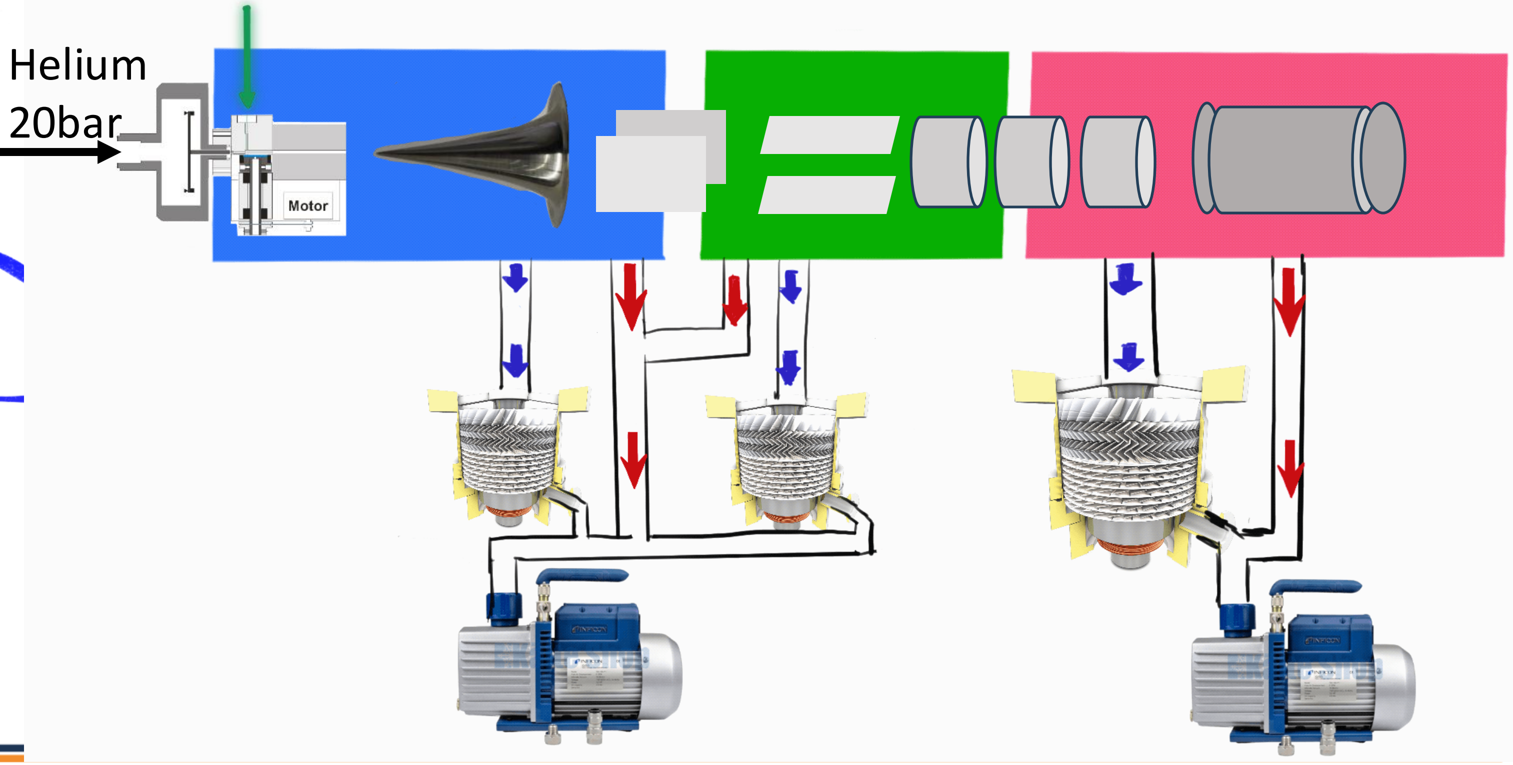

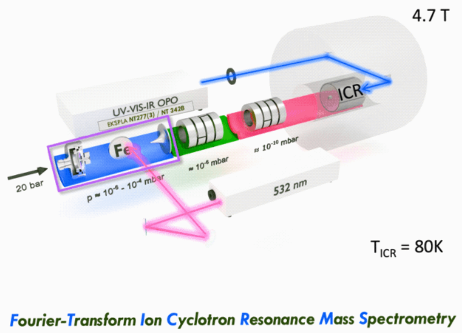

EXPERIMENTAL SETUP - Detection

$Eq = \frac{1}{2} mv^2$

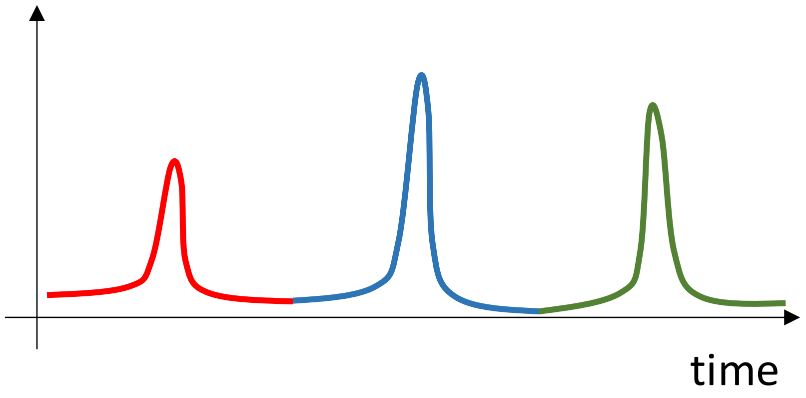

Wiley McLaren Time of Flight

EXPERIMENTAL SETUP - Detection

$$\omega_c = \frac{qB}{m}$$

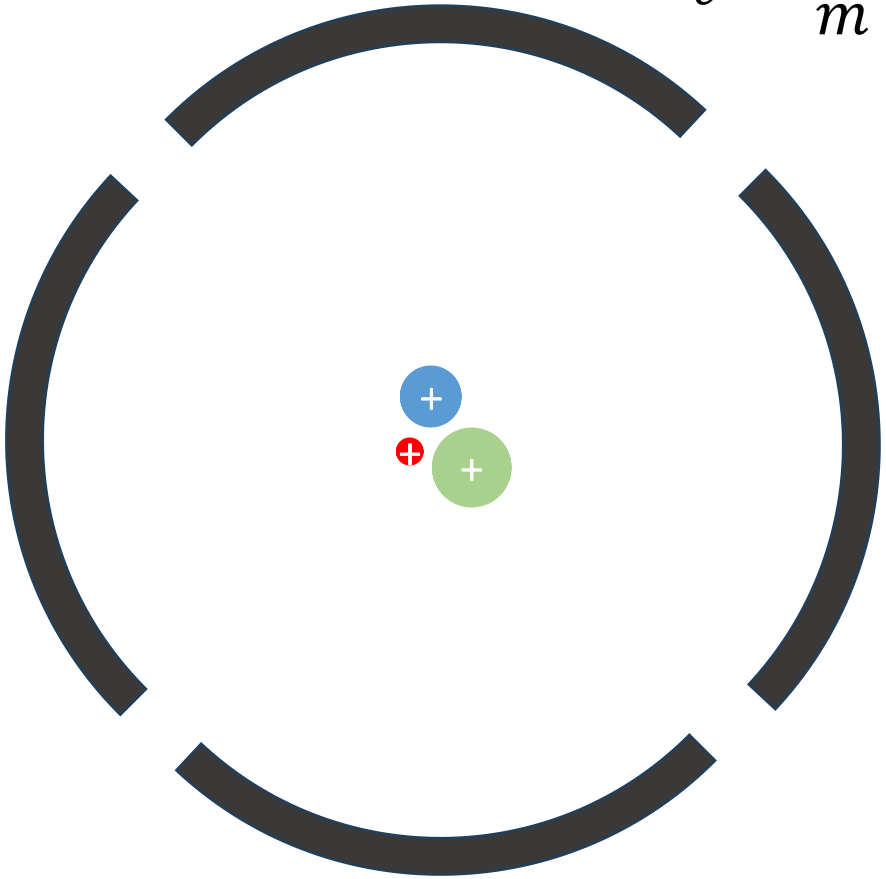

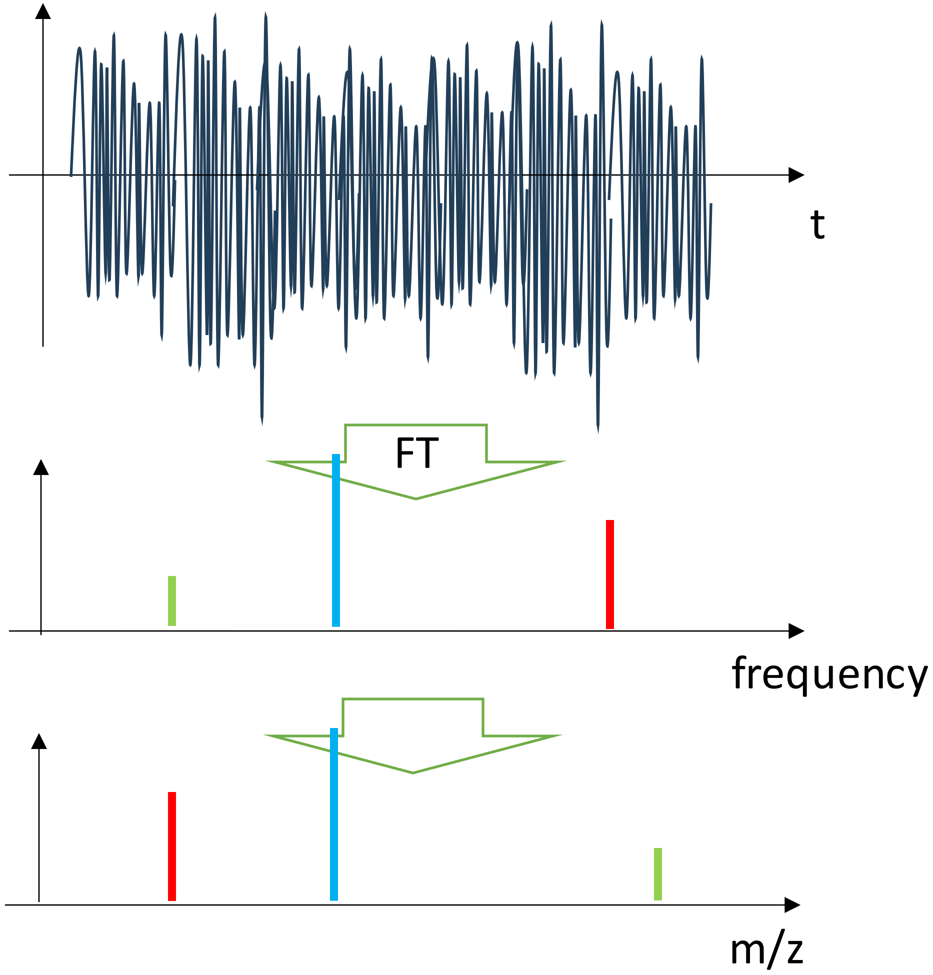

EXPERIMENTAL SETUP – OPO

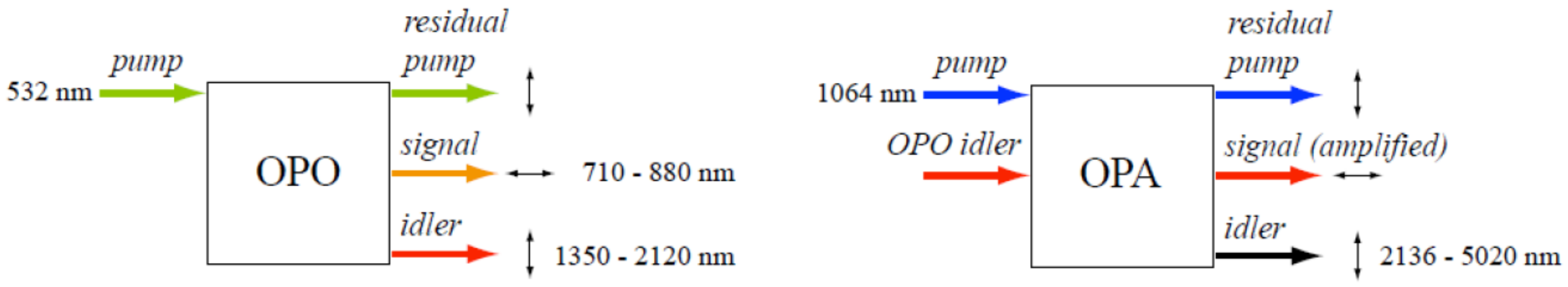

EXPERIMENTAL SETUP

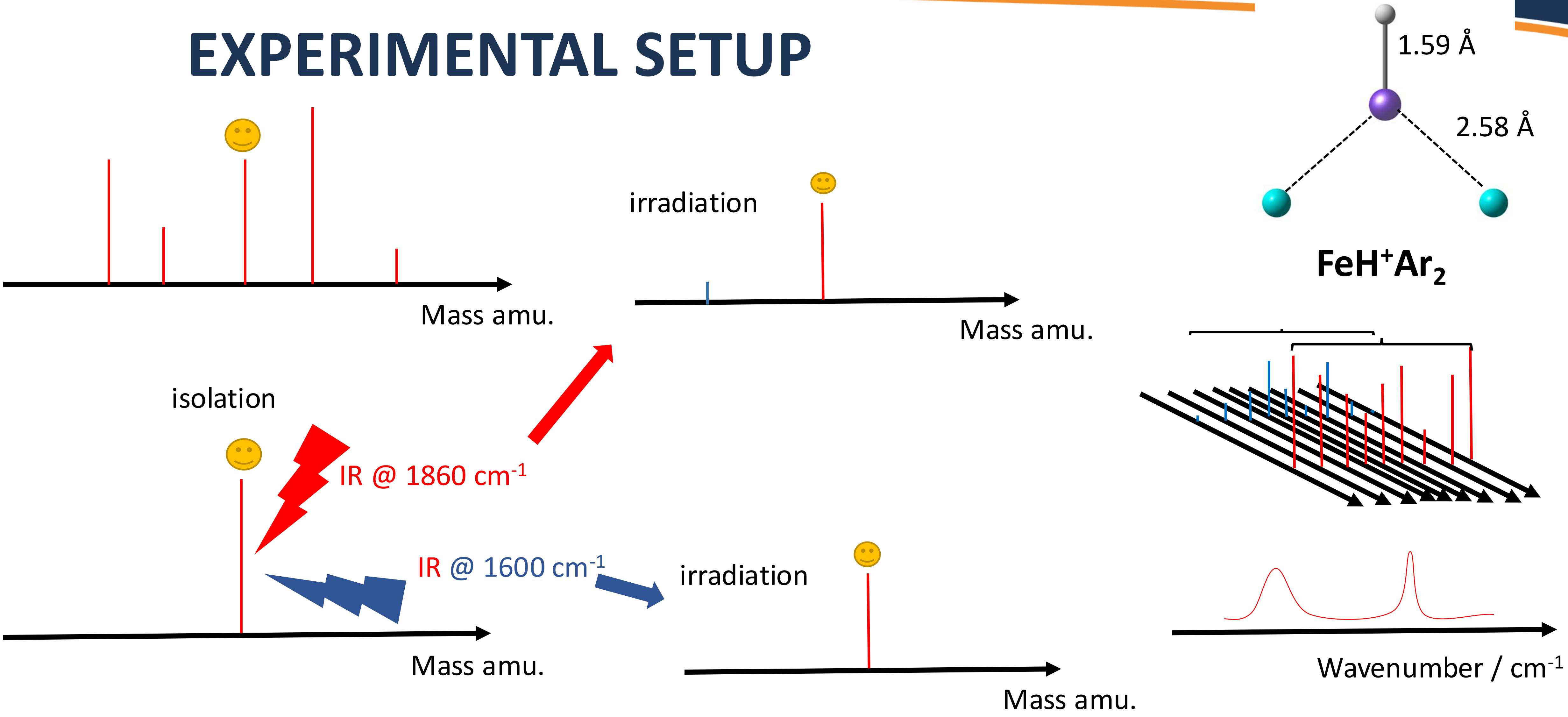

RESULTS

FeH^+: Structure and Tagging

1.59 Å

– H

Δ*E* = 208 kJ/mol

(Exp.: 205 ± 6 kJ/mol)[1]

FeH^+ **Fe^+**

$C_{\infty v}$

CCSD/aug-cc-pVTZ

S. Jin, J. Heller, C. van der Linde, MO, M. K. Beyer.
J. Phys. Chem. Lett. 13, 5867–5872 (2022).

[1] – J. L. Elkind, P. B. Armentrout,
J. Phys. Chem. 90, 5736–5745 (1986).

FeH^+: Structure and Tagging

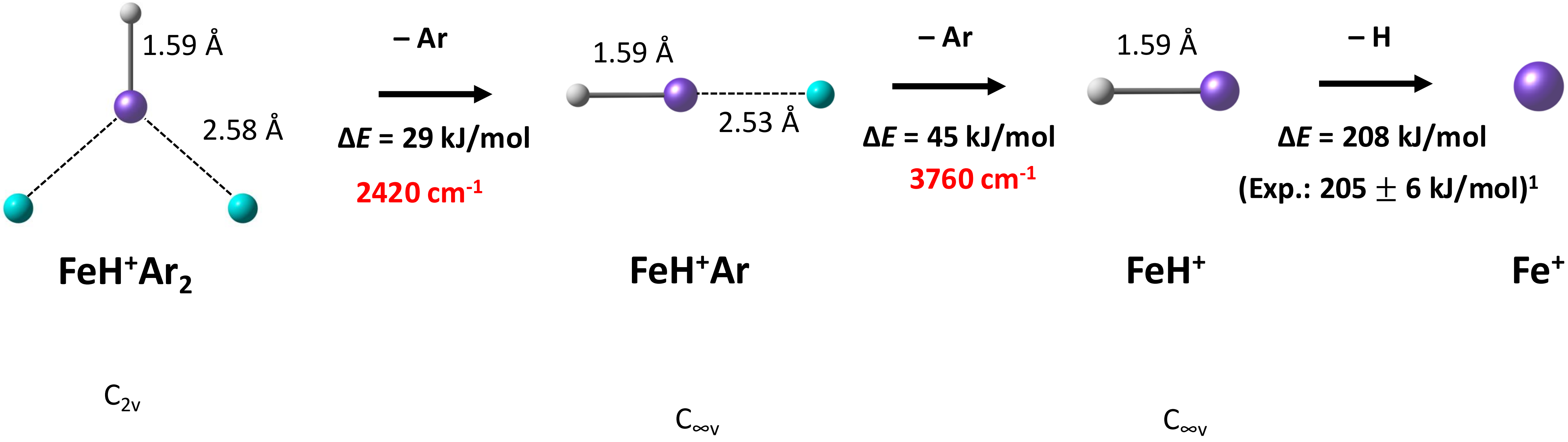

CCSD/aug-cc-pVTZ

S. Jin, J. Heller, C. van der Linde, MO, M. K. Beyer. *J. Phys. Chem. Lett. 13*, 5867–5872 (2022).

[1] – J. L. Elkind, P. B. Armentrout, *J. Phys. Chem. 90*, 5736–5745 (1986).

Ar_2FeH^+

Symmetry Breaking through Tagging

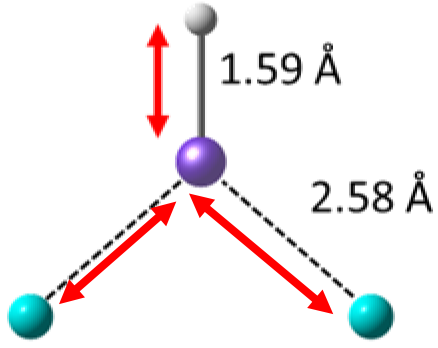

FeH^+Ar_2

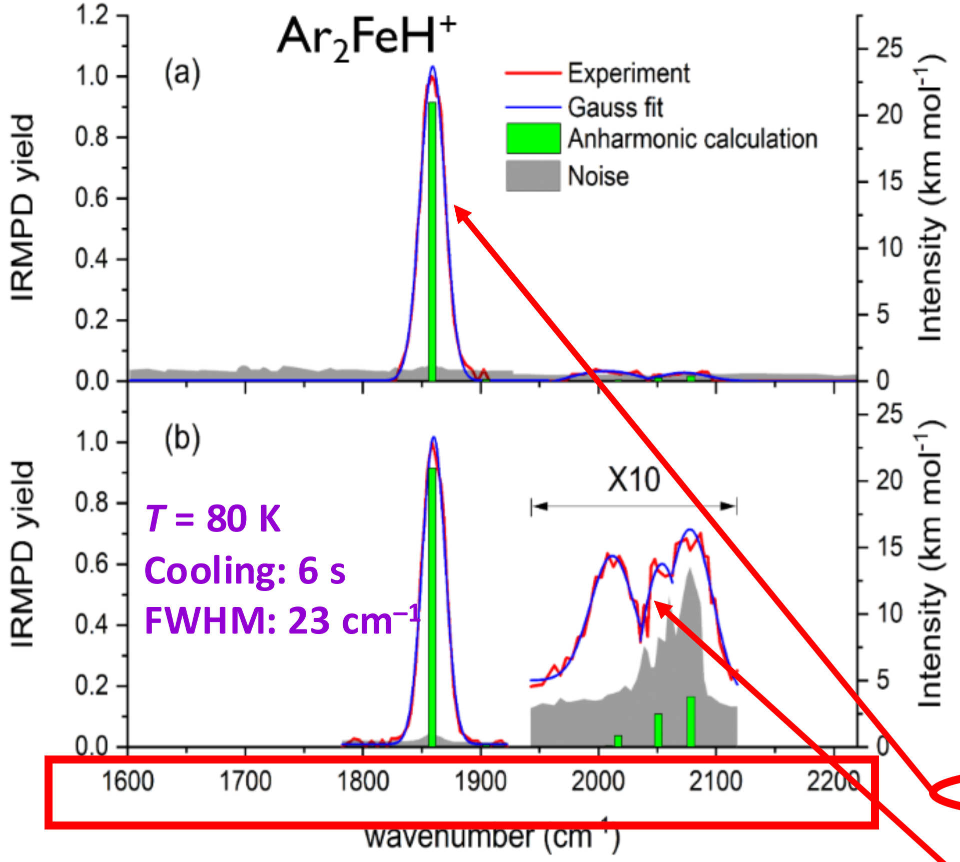

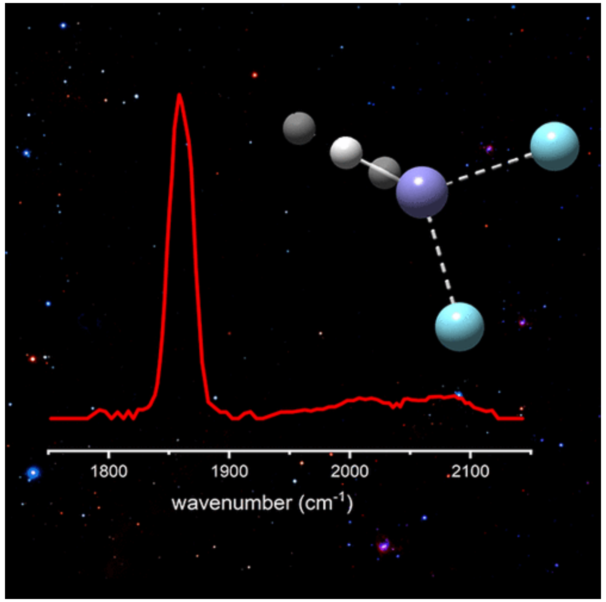

J. Phys. Chem. Lett. **2022**, 13, 25, 5867–5872

$Ar_2FeH^+ + mh\nu \rightarrow ArFeH^+ + Ar$

ΔE = 29 kJ/mol
~2420 cm^{-1}

Expt.	mode	theory		
Ar_2FeH^+		Ar_2FeH^+	$ArFeH^+$	FeH^+
1860	$\tilde{\nu}_1$	1862 (21.07)	1878 (9.94)	1793 (1.89)
2078	$\tilde{\nu}_1 + \tilde{\nu}_2$	2090 (0.38)		
2054	$\tilde{\nu}_1 + \tilde{\nu}_3$	2061 (0.25)		
2012	$\tilde{\nu}_1 + \tilde{\nu}_4$	2014 (0.09)		

Anharmonic frequency analysis B3LYP-D3/aug-cc-pVTZ

FeH^+Ar_2: IR Spectrum

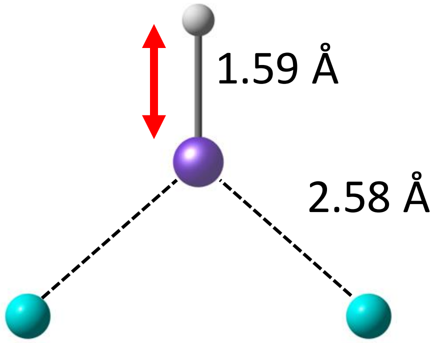

FeH^+Ar_2

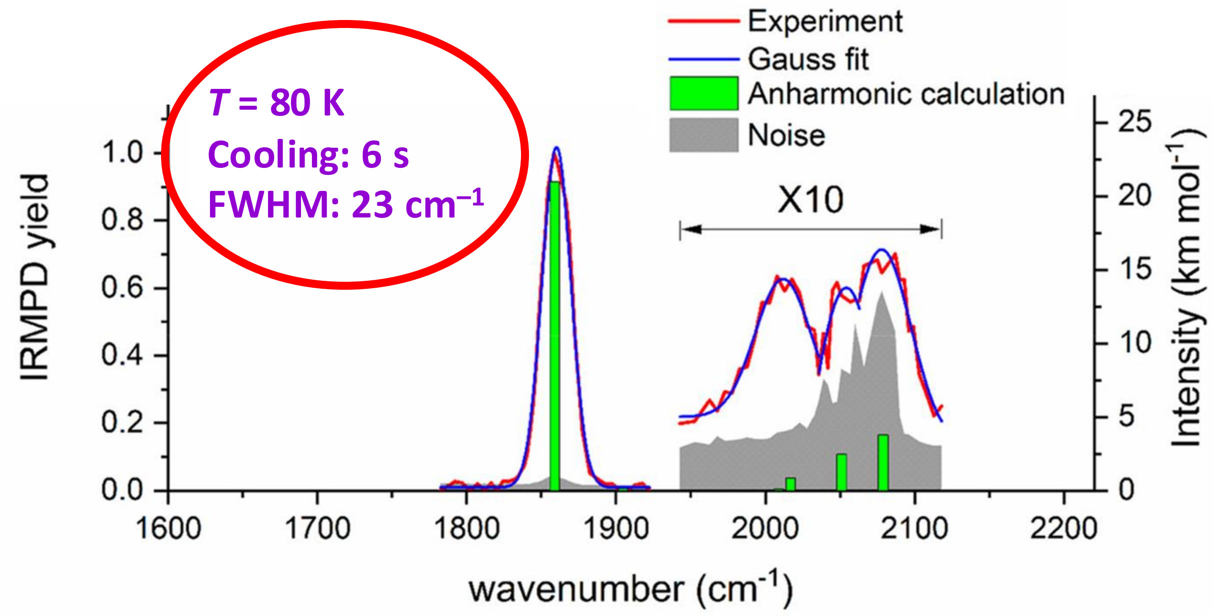

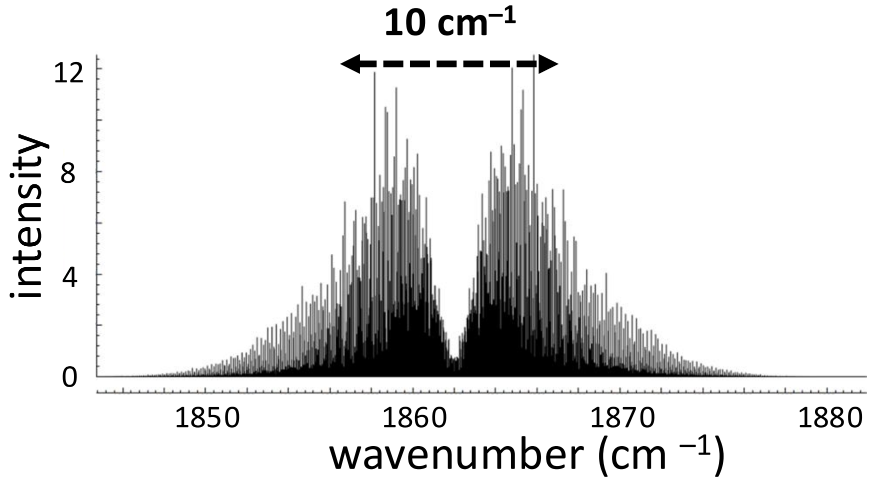

S. Jin, J. Heller, C. van der Linde, MO, M. K. Beyer.
J. Phys. Chem. Lett. 13, 5867–5872 (2022).

optimization: CCSD/aug-cc-pVTZ;
frequencies: B3LYP-D3/aug-cc-pVTZ

FeH^+Ar_2: IR Spectrum

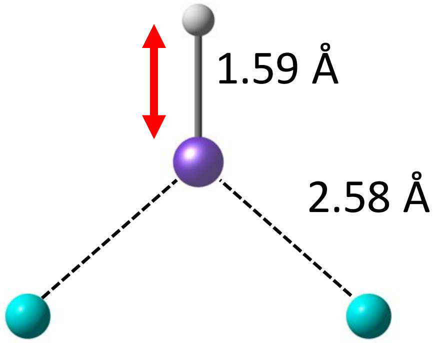

FeH^+Ar_2

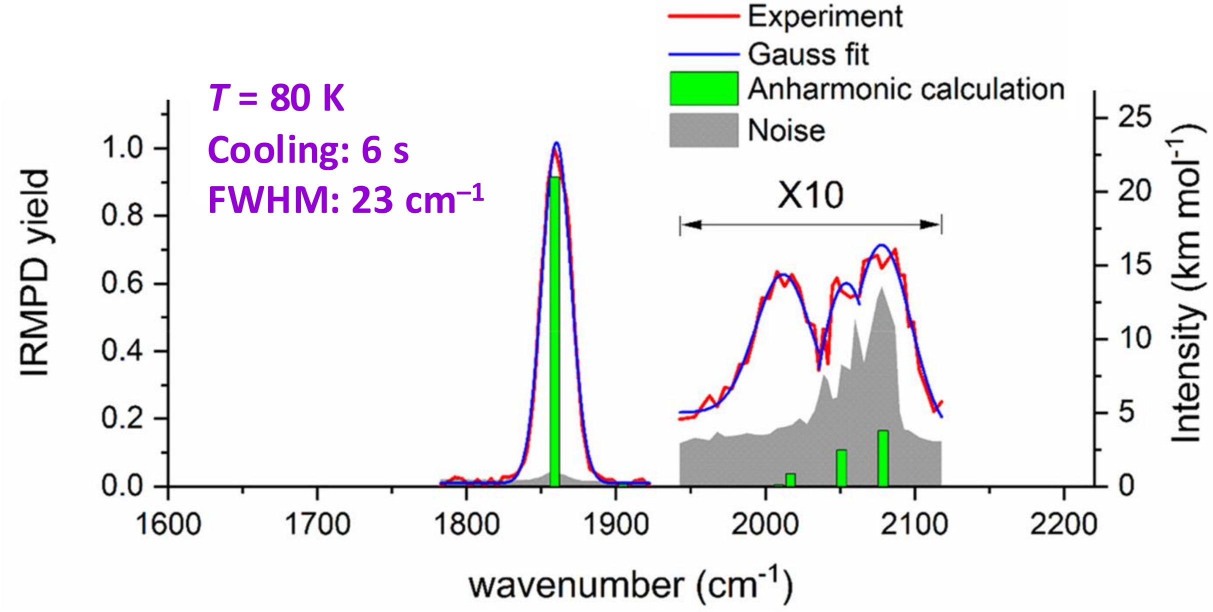

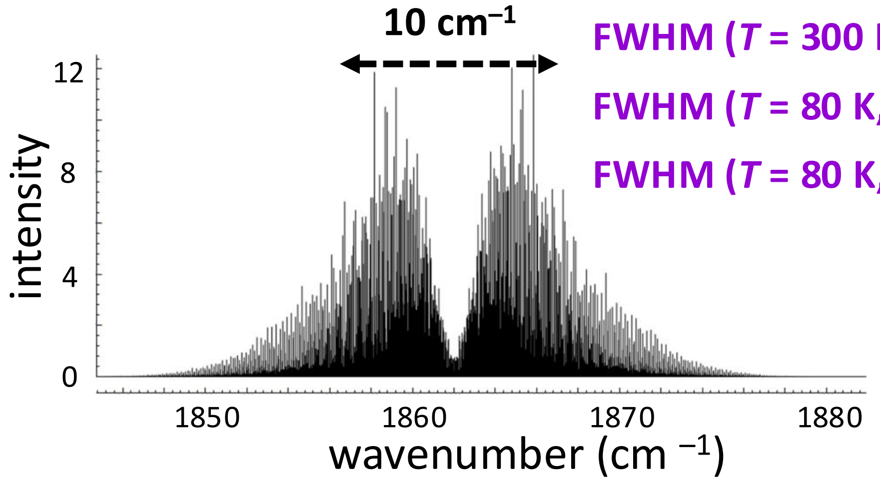

FWHM (T = 300 K): 30 cm^{-1}

FWHM (T = 80 K, 3 s cooling): 25 cm^{-1}

FWHM (T = 80 K, 6 s cooling): 23 cm^{-1}

S. Jin, J. Heller, C. van der Linde, MO, M. K. Beyer. *J. Phys. Chem. Lett.* 13, 5867–5872 (2022).

optimization: CCSD/aug-cc-pVTZ;
frequencies: B3LYP-D3/aug-cc-pVTZ

FeH^+Ar_2: IR Spectrum

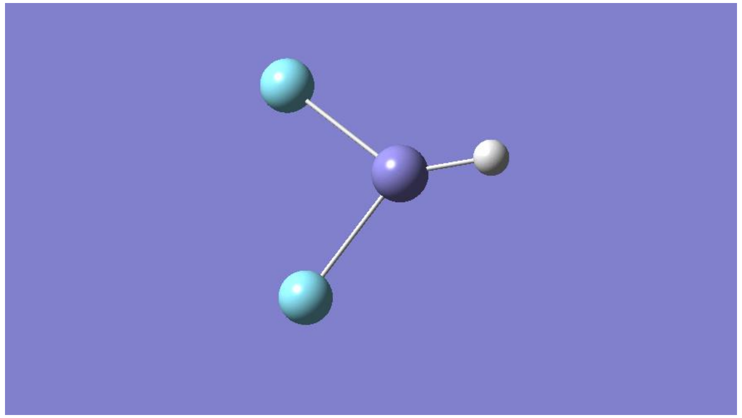

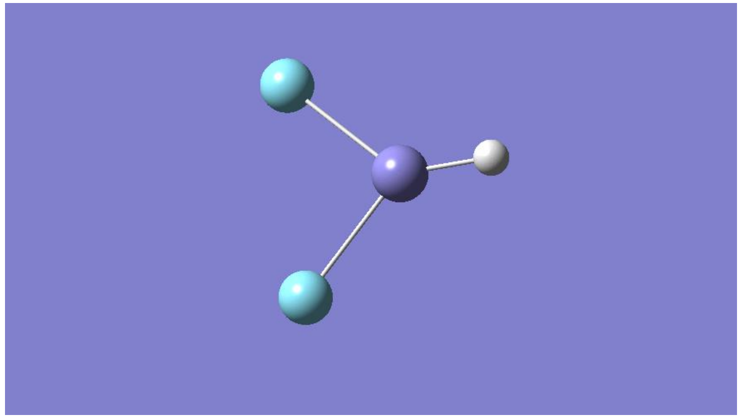

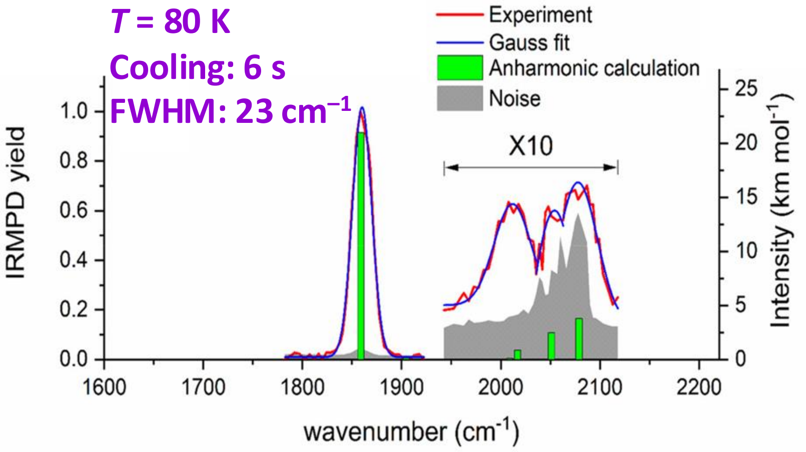

$\nu_{Ar\text{-}Fe\text{-}Ar}$ = 46 cm^{-1}

$\nu_{Fe\text{-}H}$ = 1906 cm^{-1}

S. Jin, J. Heller, C. van der Linde, M. Ončák, M. K. Beyer.
J. Phys. Chem. Lett. 13, 5867–5872 (2022).

optimization: CCSD/aug-cc-pVTZ;
frequencies: CCSD/aug-cc-pVTZ

FeH^+Ar_2: IR Spectrum

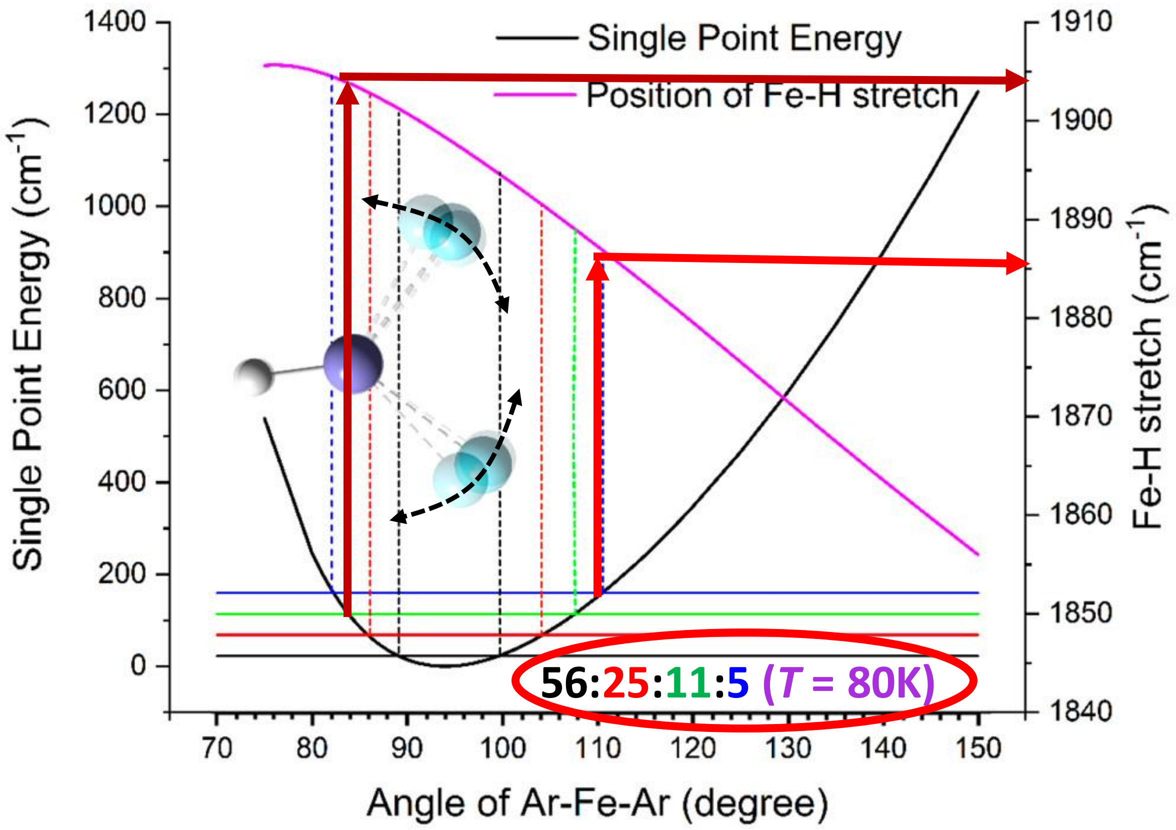

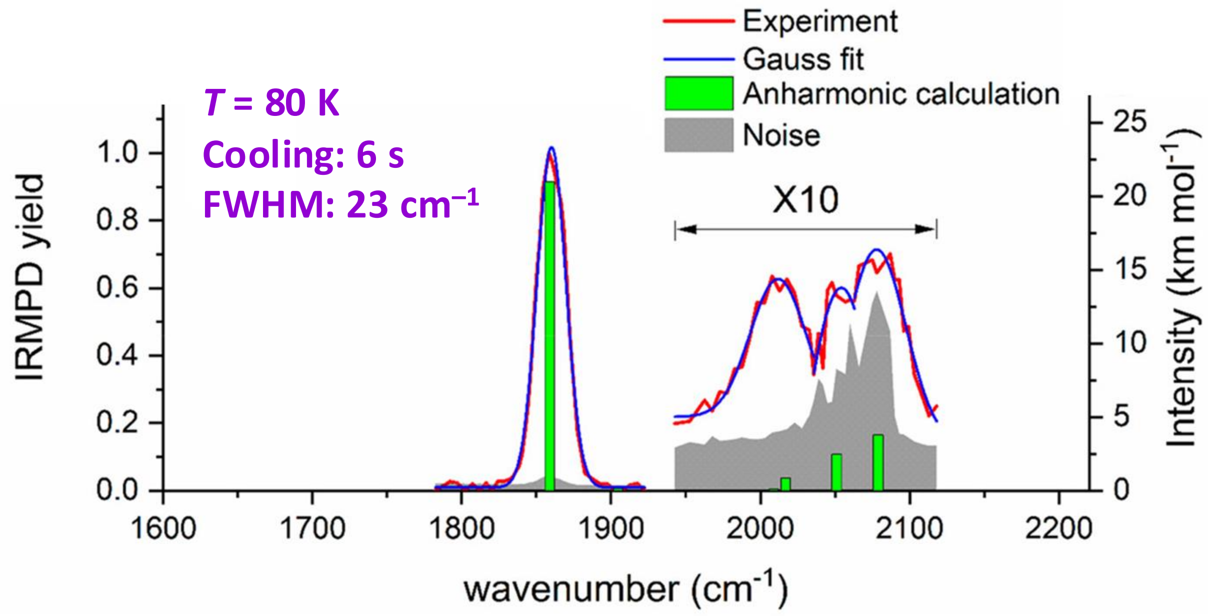

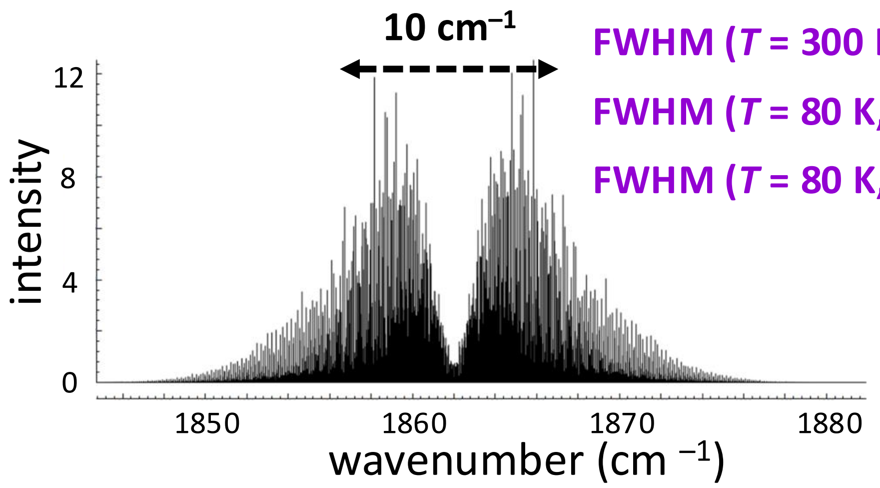

FWHM (*T* = 300 K): 30 cm–1

FWHM (*T* = 80 K, 3 s cooling): 25 cm–1

FWHM (*T* = 80 K, 6 s cooling): 23 cm–1

universität innsbruck

S. Jin, J. Heller, C. van der Linde, MO, M. K. Beyer. *J. Phys. Chem. Lett.* 13, 5867–5872 (2022).

optimization: CCSD/aug-cc-pVTZ;
frequencies: B3LYP-D3/aug-cc-pVTZ

$Ar_{1,2}FeH(D)^+$ and overtone study

Experimental IRMPD spectra

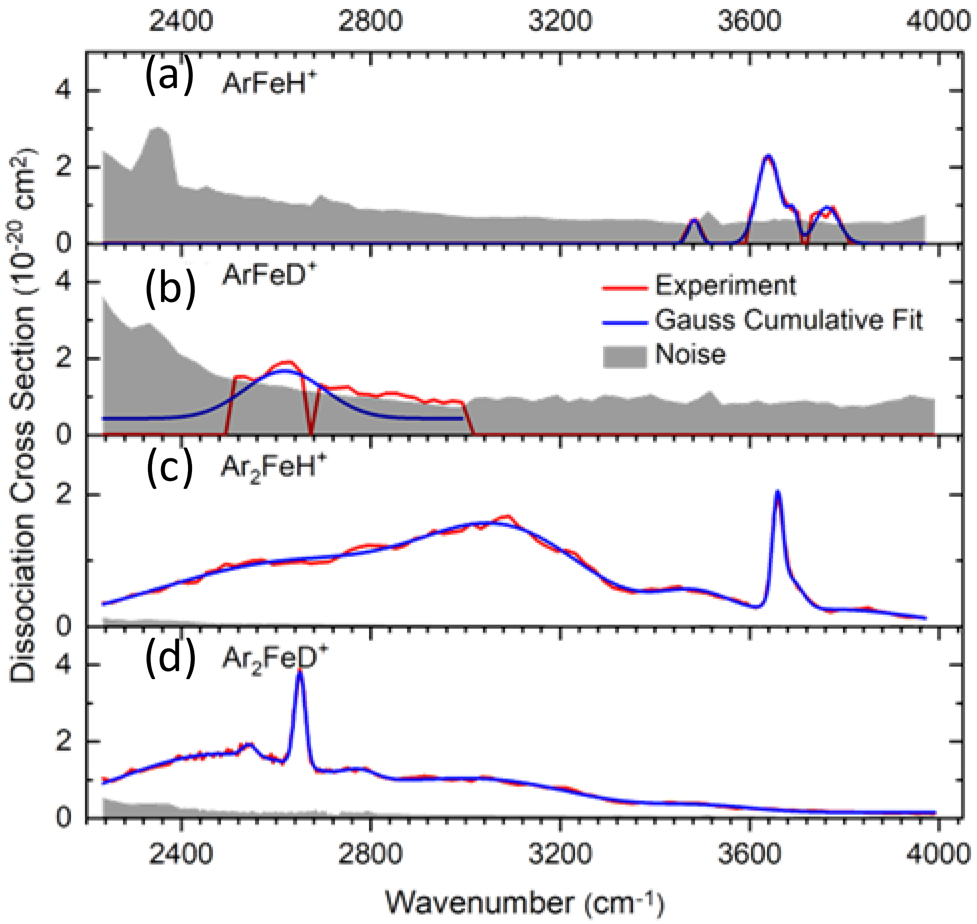

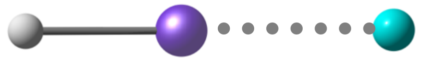

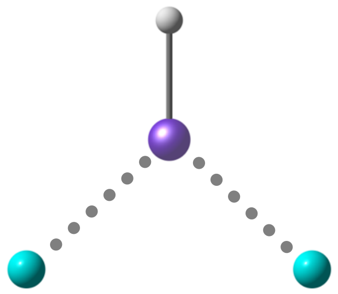

Besides deuteration, argon tagging also leads to a shift of the spectral band positions!

$Ar_{1,2}FeH(D)^+$ and overtone study

Fe (K_h)

FeH^+ ($C_{\infty v}$)

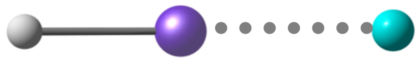

FeH^+Ar ($C_{\infty v}$)

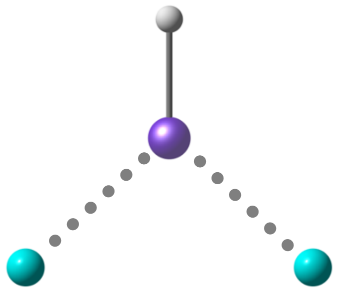

FeH^+Ar_2 (C_{2v})

$Ar_{1,2}FeH(D)^+$ and overtone study

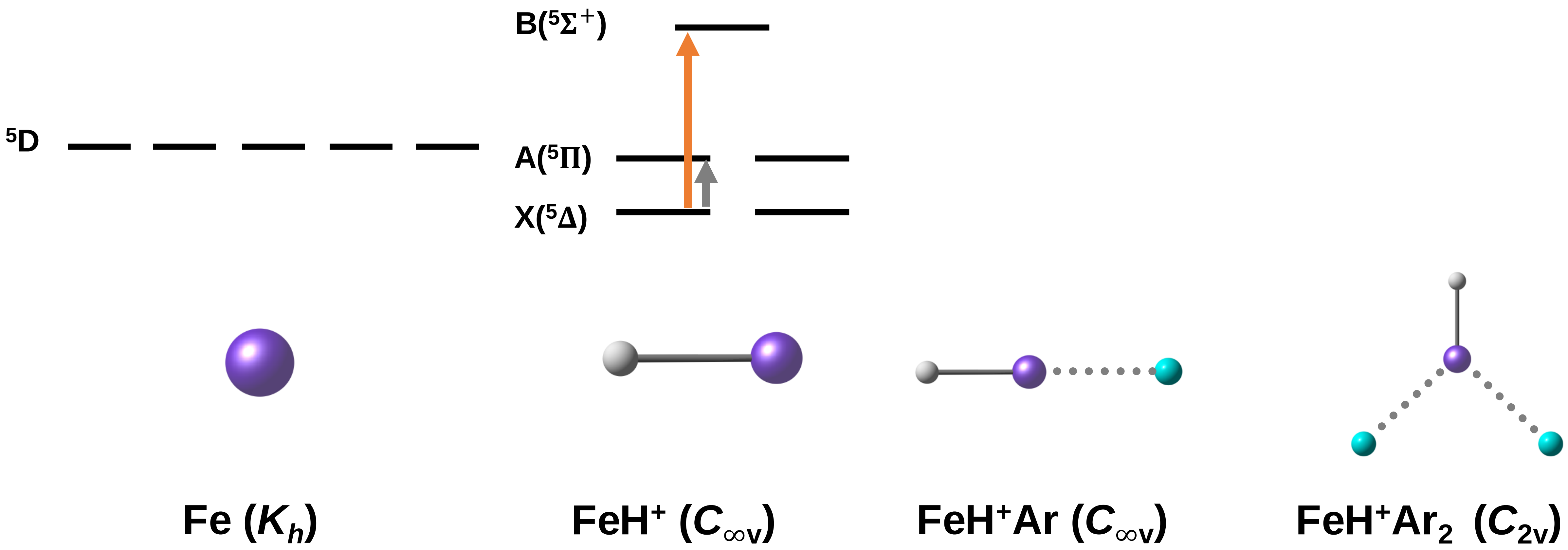

Stephen R Langhoff, Charles W Bauschlicher Jr. Astrophzsical Journal, 375:843-845,1991

$Ar_{1,2}FeH(D)^+$ and overtone study

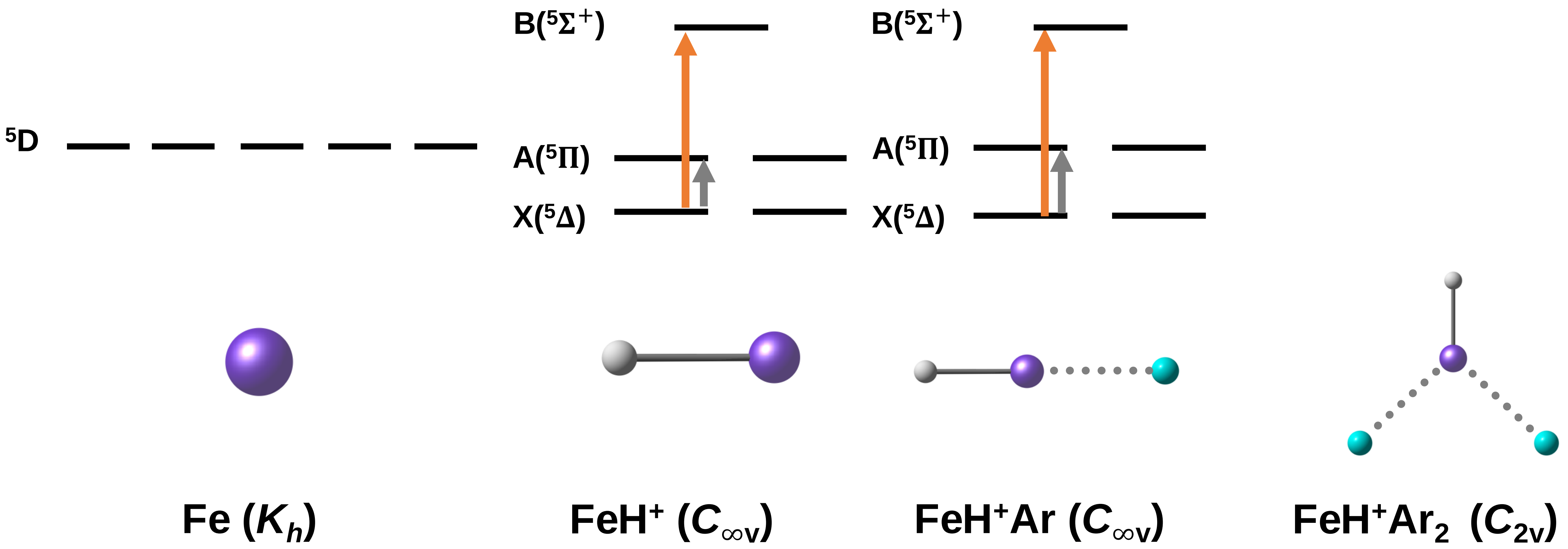

$Ar_{1,2}FeH(D)^+$ and overtone study

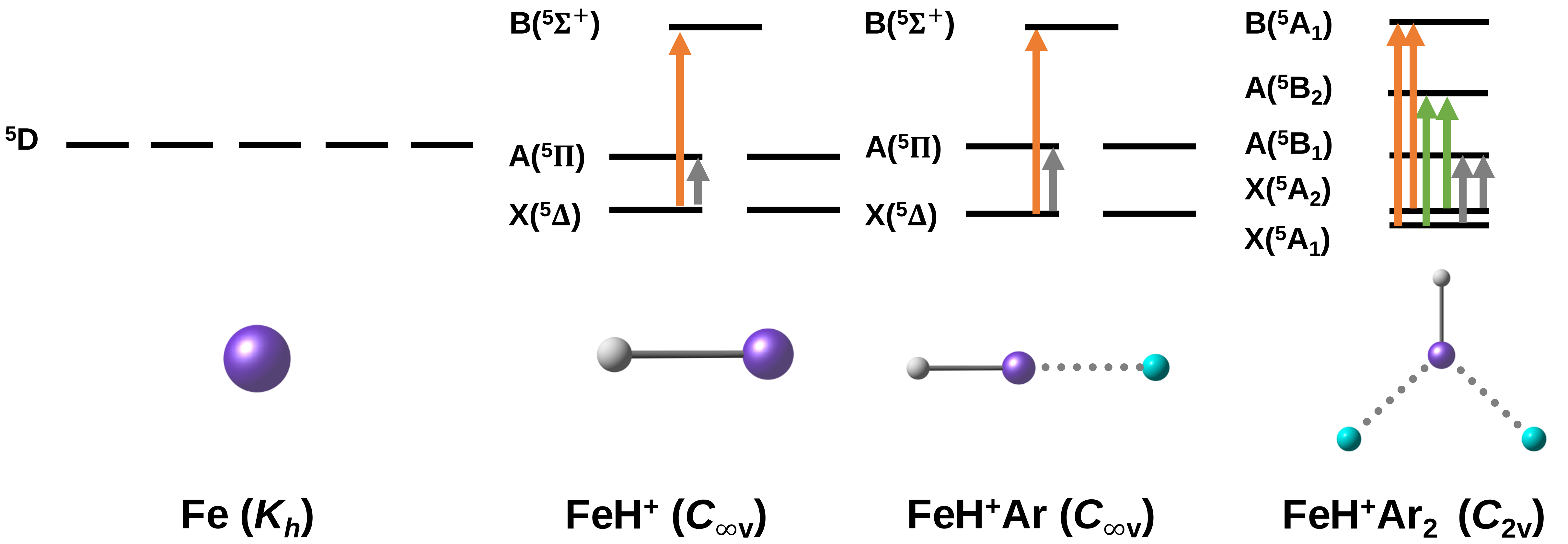

$Ar_{1,2}FeH(D)^+$ and overtone study

(v = 0→2)

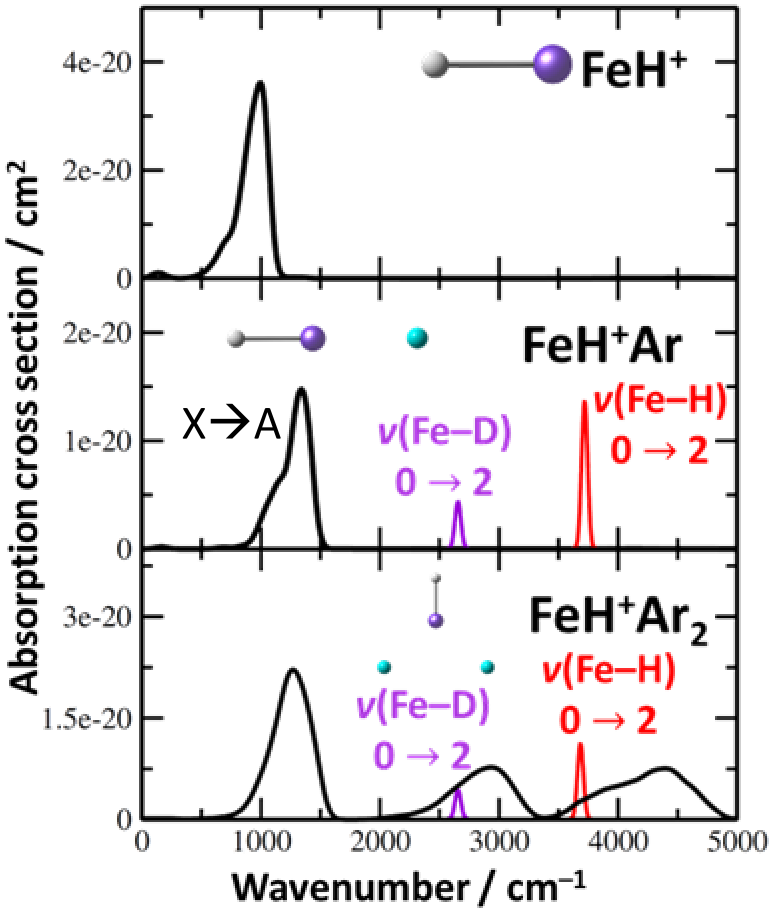

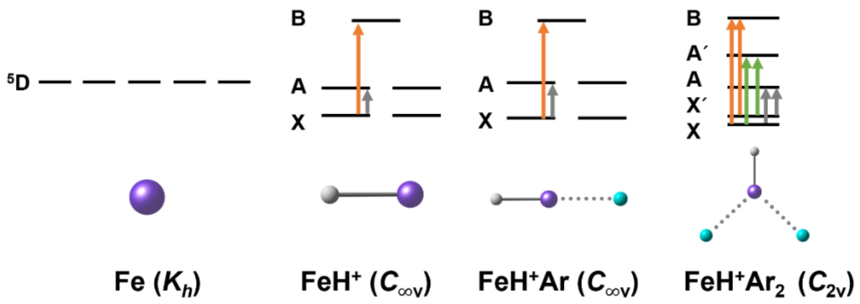

*Splitting of the ^5D term in iron upon addition of **H^+** and complexation with **Ar** Symmetrically allowed*

Milan Ončák, Lukáš Šištík, Petr Slavíček. J. Chem. Phys. 133, 174303 (2010).

MRCI(8,7)+SO/aug-cc-pVDZ, reflection principle freq: B3LYP-D3/aug-cc-pVTZ

$Ar_{1,2}FeH(D)^+$ and overtone study

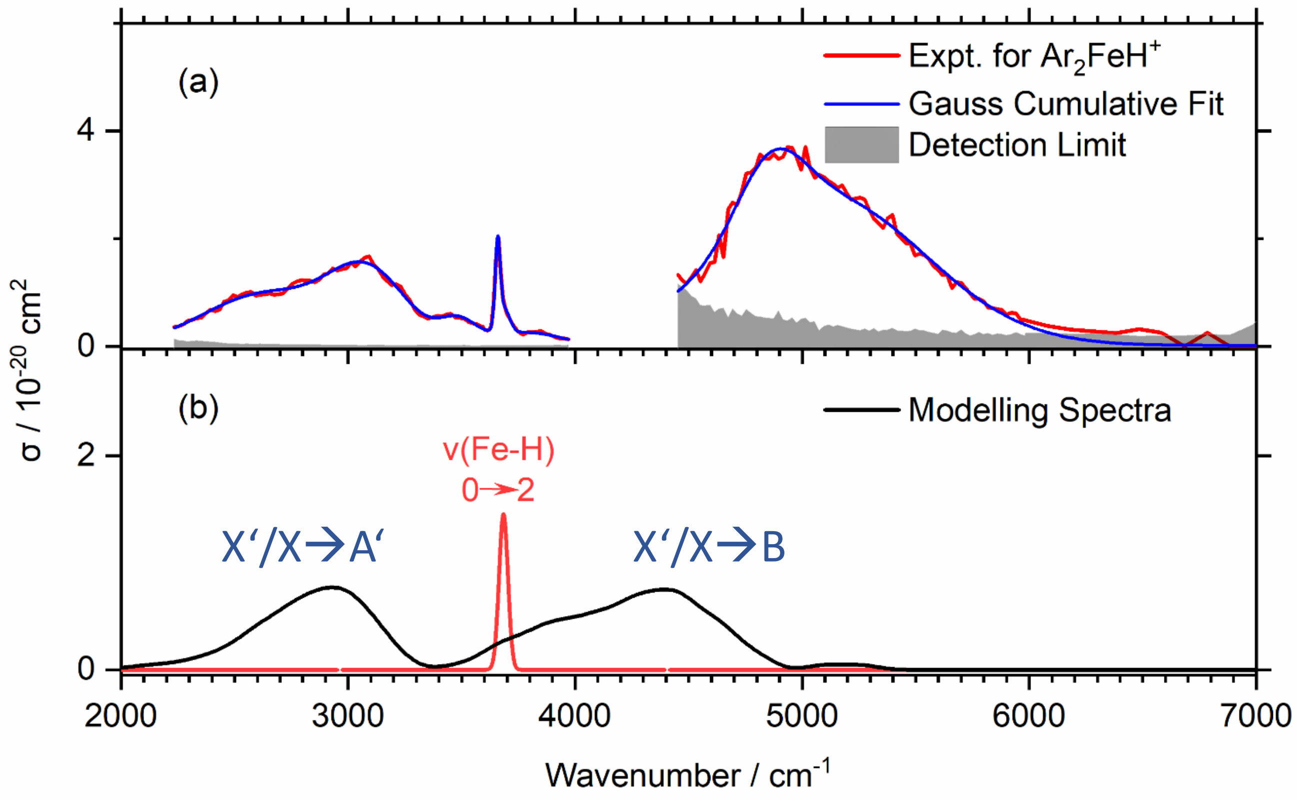

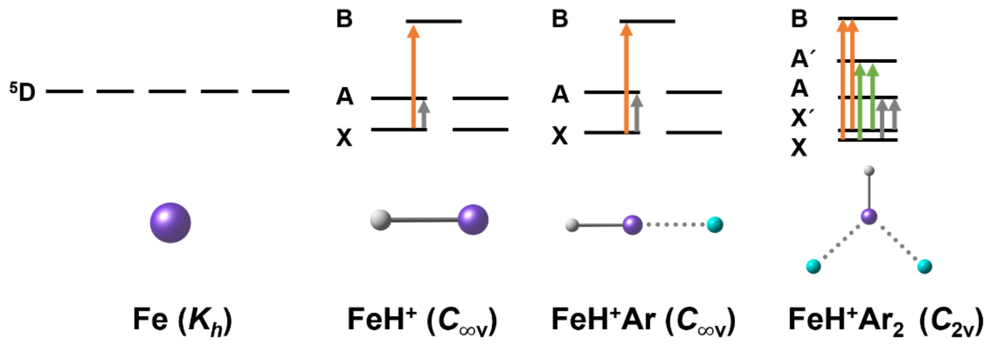

MRCI(8,7)+SO/aug-cc-pVDZ, reflection principle freq: B3LYP-D3/aug-cc-pVTZ

FeH^+: X-ray Spectrum

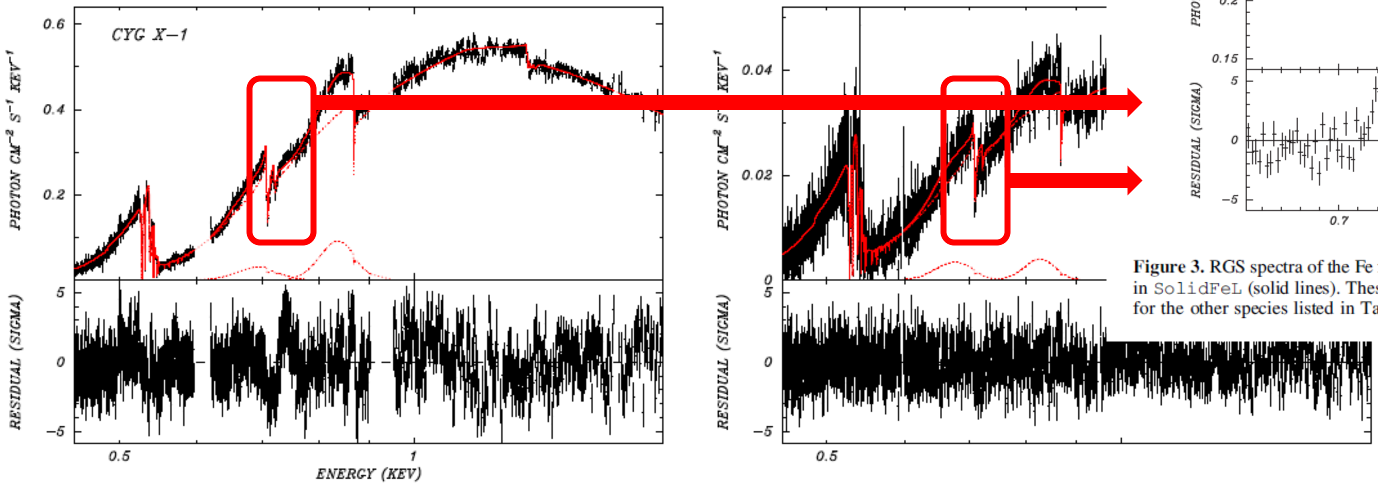

Figure 2. The RGS spectra (crosses) for Cygnus X-1 (left) and GX 339-4 (right) using the paramete
uncertainty, and the horizontal the energy bin widths. In each upper panel, the best-fit continuum mo
model components. The lower panels show the residuals from the fitted model in units of σ. The ga
RGS CCD detectors covering those dispersed wavelengths.

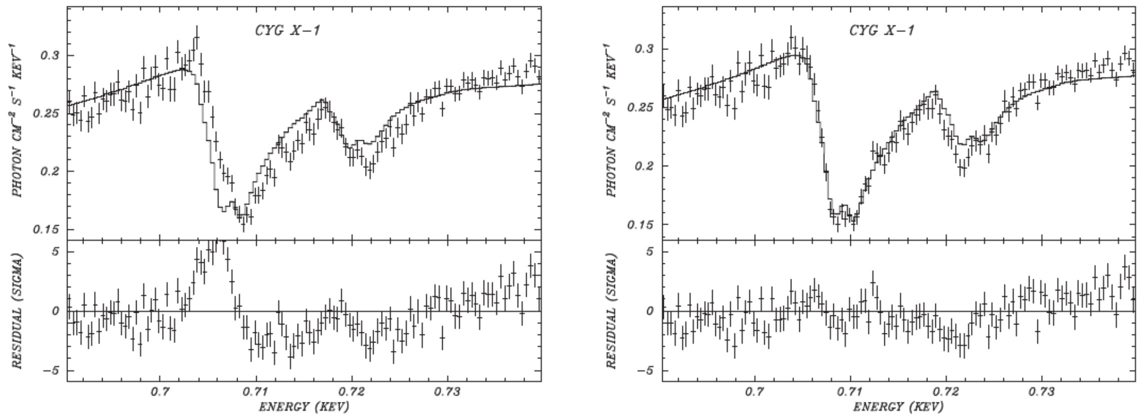

Figure 3. RGS spectra of the Fe feature in Cygnus X-1 fitted in the 0.69–0.74 keV energy range with the (left) unshifted and (right) shifted (+1.88 eV) fayalite model in `SolidFeL` (solid lines). These panels highlight the evidence for an energy offset error in the published experimental cross section data. Similar results are found for the other species listed in Table 1.

Table 6
Narrowband Spectral Fits to the Fe *L*-shell Features in the Two ISM Sight Lines Probed

`SolidFeL` Compound *i*	Formula	Cygnus X-1 ΔE_{shift} (eV)	Cygnus X-1 $M_{d,i}$ (10^{-4} g cm^{-2})	Cygnus X-1 C_{stat} (dof = 119)	GX 339-4 ΔE_{shift} (eV)	GX 339-4 $M_{d,i}$ (10^{-4} g cm^{-2})	GX 339-4 C_{stat} (dof = 119)
Lepidocrocite	γ-FeOOH	1.14 ± 0.26	0.301 ± 0.022	201.1	1.04 ± 0.61	0.349 ± 0.047	145.1
Hematite	α-Fe_2O_3	1.21 ± 0.26	0.320 ± 0.022	211.0	1.10 ± 0.61	0.376 ± 0.050	145.2
Fayalite	Fe_2SiO_4	1.88 ± 0.27	0.277 ± 0.019	216.3	1.80 ± 0.63	0.318 ± 0.043	143.9
Ferrous Sulfate	$FeSO_4$	2.32 ± 0.26	0.394 ± 0.032	467.7	2.18 ± 0.59	0.533 ± 0.082	173.4
Metallic Iron	Fe	2.51 ± 0.31	0.252 ± 0.009	357.6	2.66 ± 0.71	0.290 ± 0.026	155.1

Note. The calibrated energy shift ΔE_{shift} is applied in the laboratory frame of the cross sections for each compound (see text). The mass column is from the fits to the Fe features in the 0.69–0.74 keV range using the `SolidFeL` model with the fitted 0.45–1.8 keV continuum model held fixed. Uncertainties are quoted at a 90% confidence level for one interesting parameter. Degrees of freedom (dof).

[1] Corrales et al.,The Astrophysical Journal, 965:172 (18pp), 2024

FeH$^+$: X-ray Spectrum

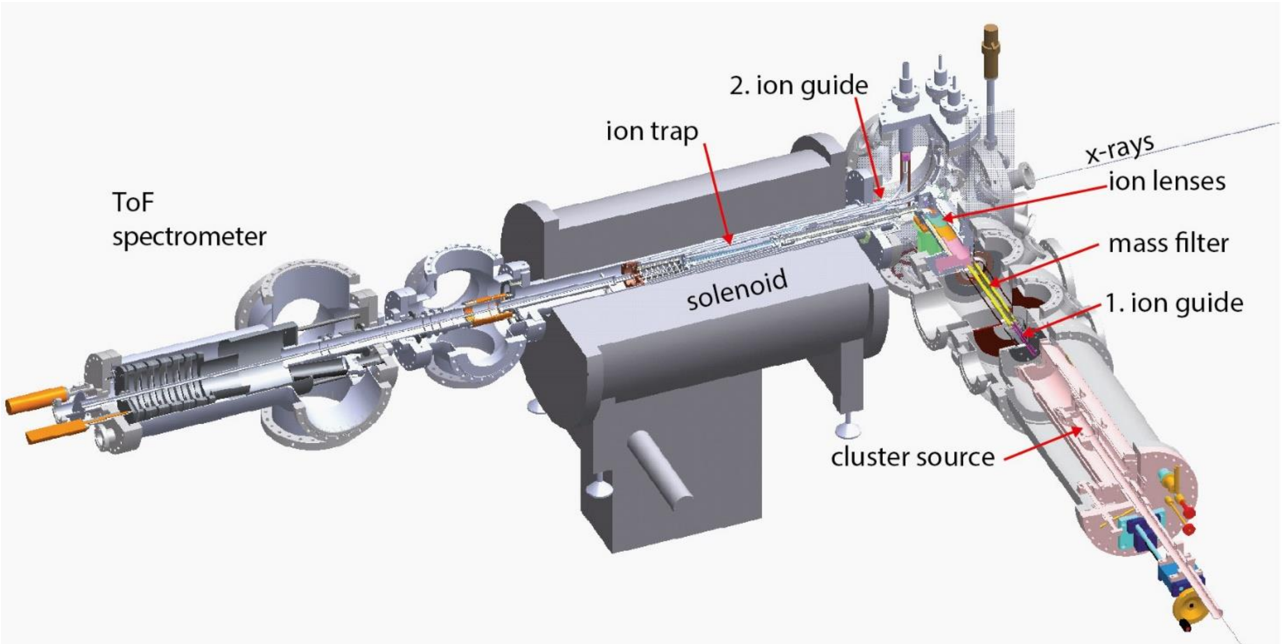

@UE52-PGM beamline

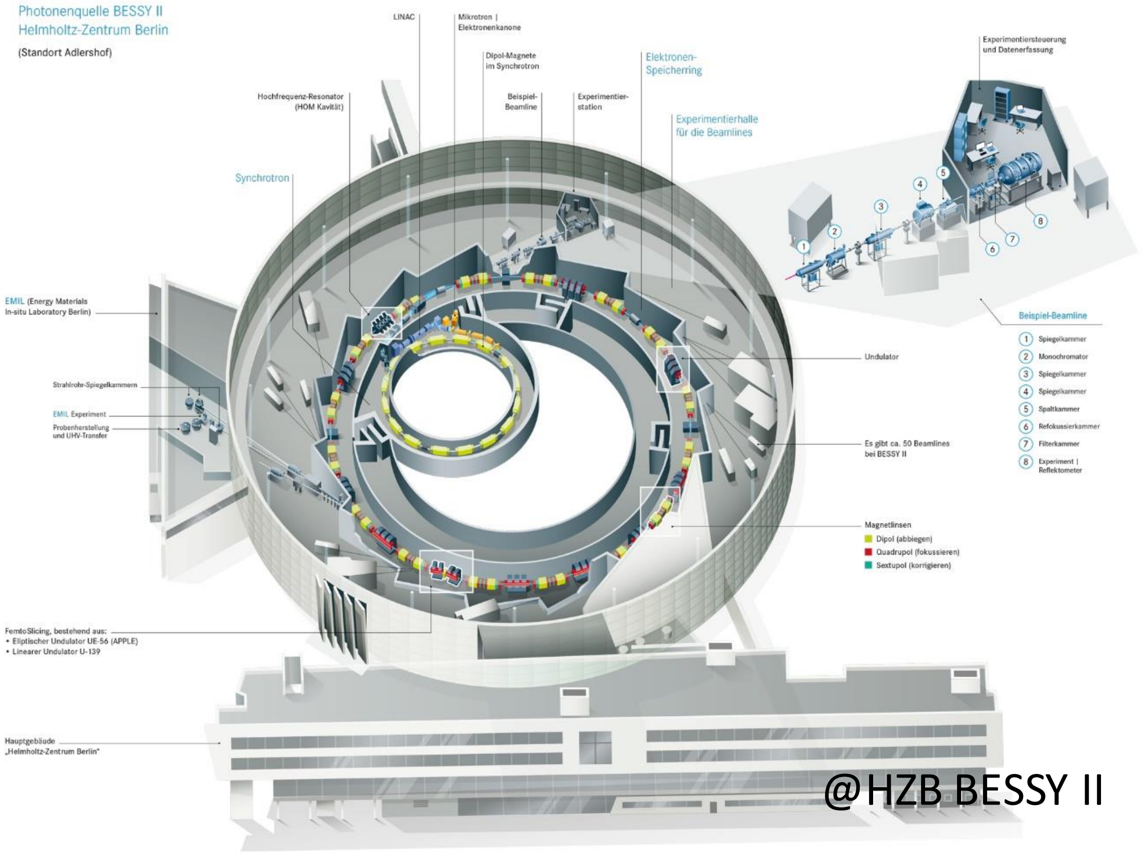

@HZB BESSY II

FeH^+: X-ray Spectrum

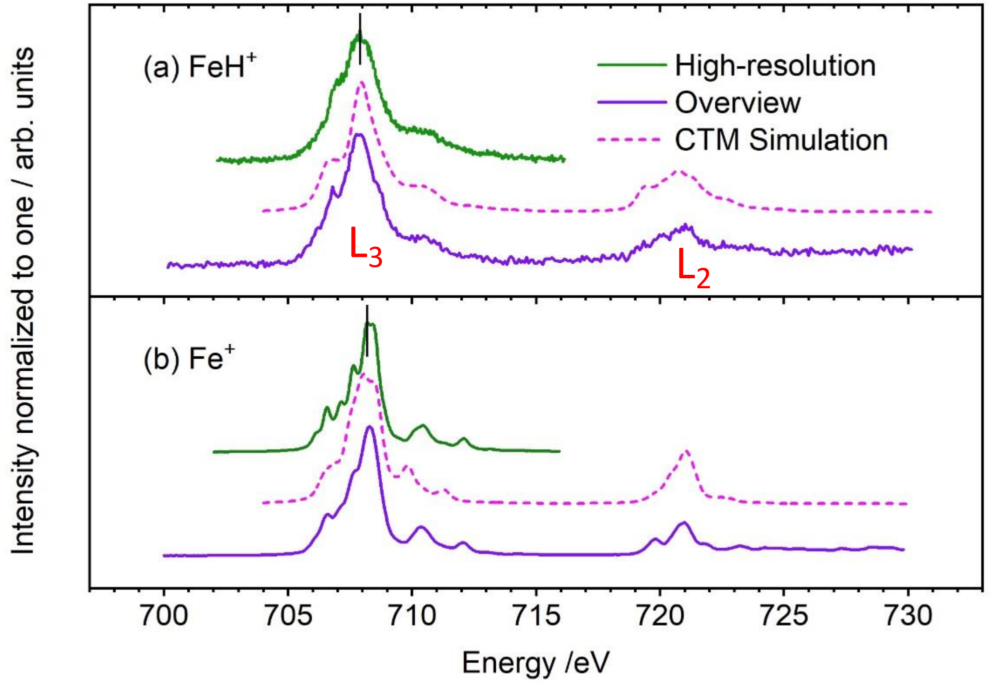

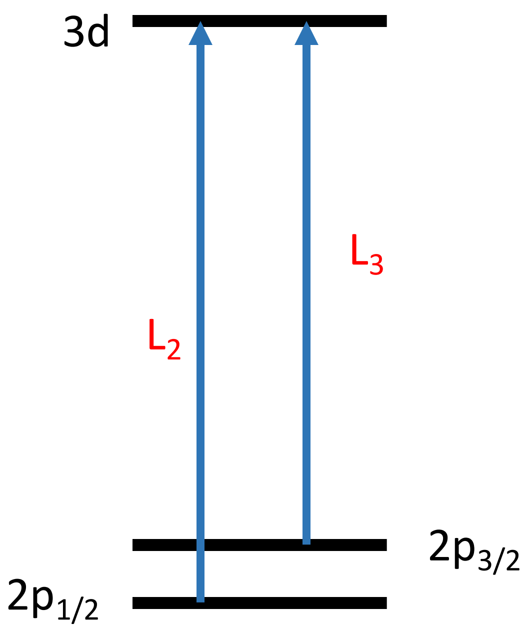

FeH^+: X-ray Spectrum

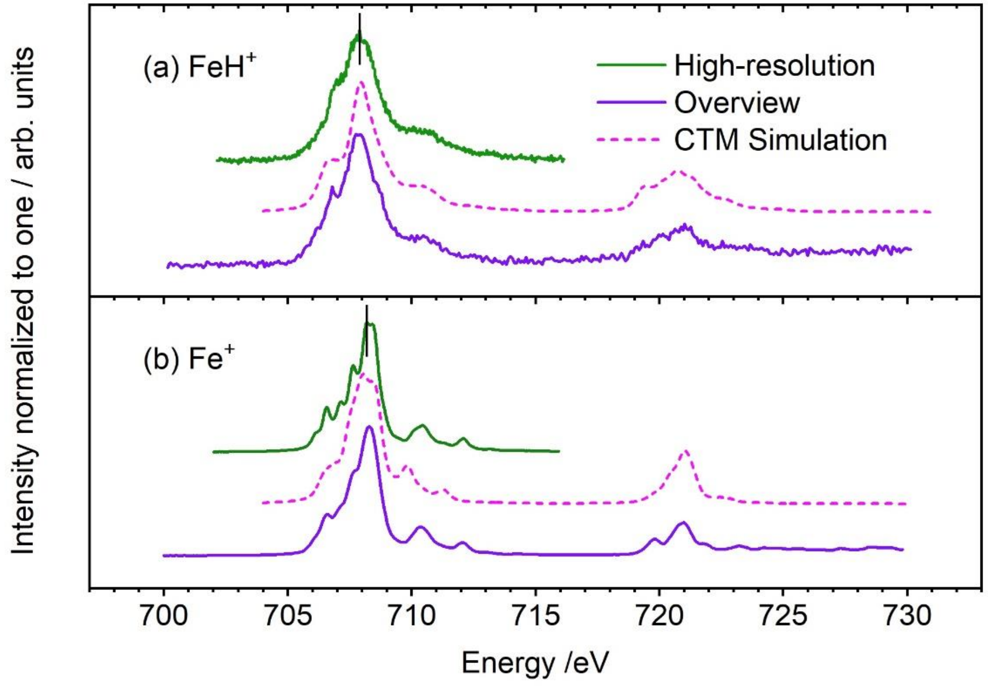

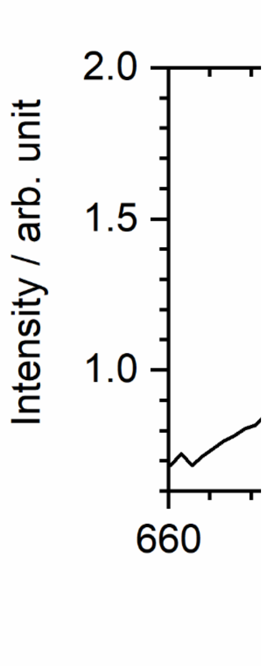

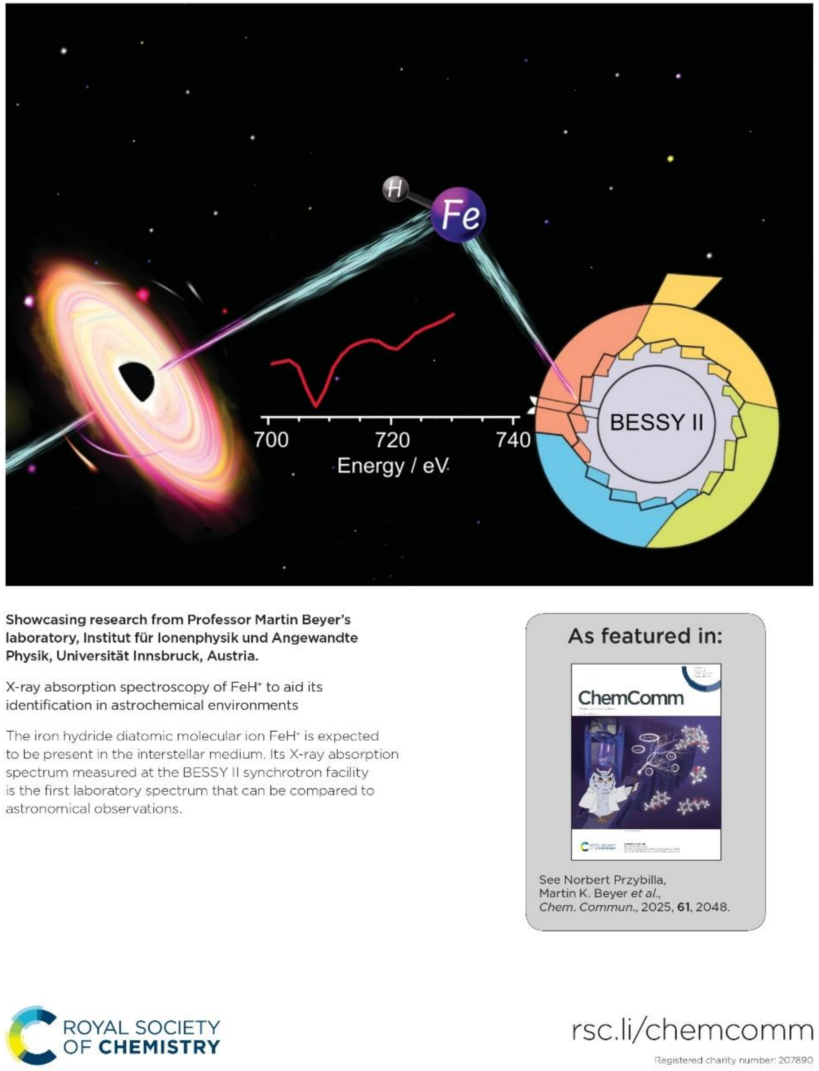

Take Home Messages

- Astrochemistry needs the **collaboration** of astrophysicists, modeling theoretical chemists, and chemical physicists (physical chemists).
- Insight into **basic principles** and **instruments** of chemical physics and physical chemistry
- Understand the spectroscopical characteristics of **Argon-tagged FeH^+,** and provides spectroscopic data first.
- First **X-ray spectroscopy of FeH^+** aids its identification in the ISM environment.

Thank Prof. Dr. Martin Beyer, Assoz. Prof. Dr. Milan Ončák, and groups' help

SI

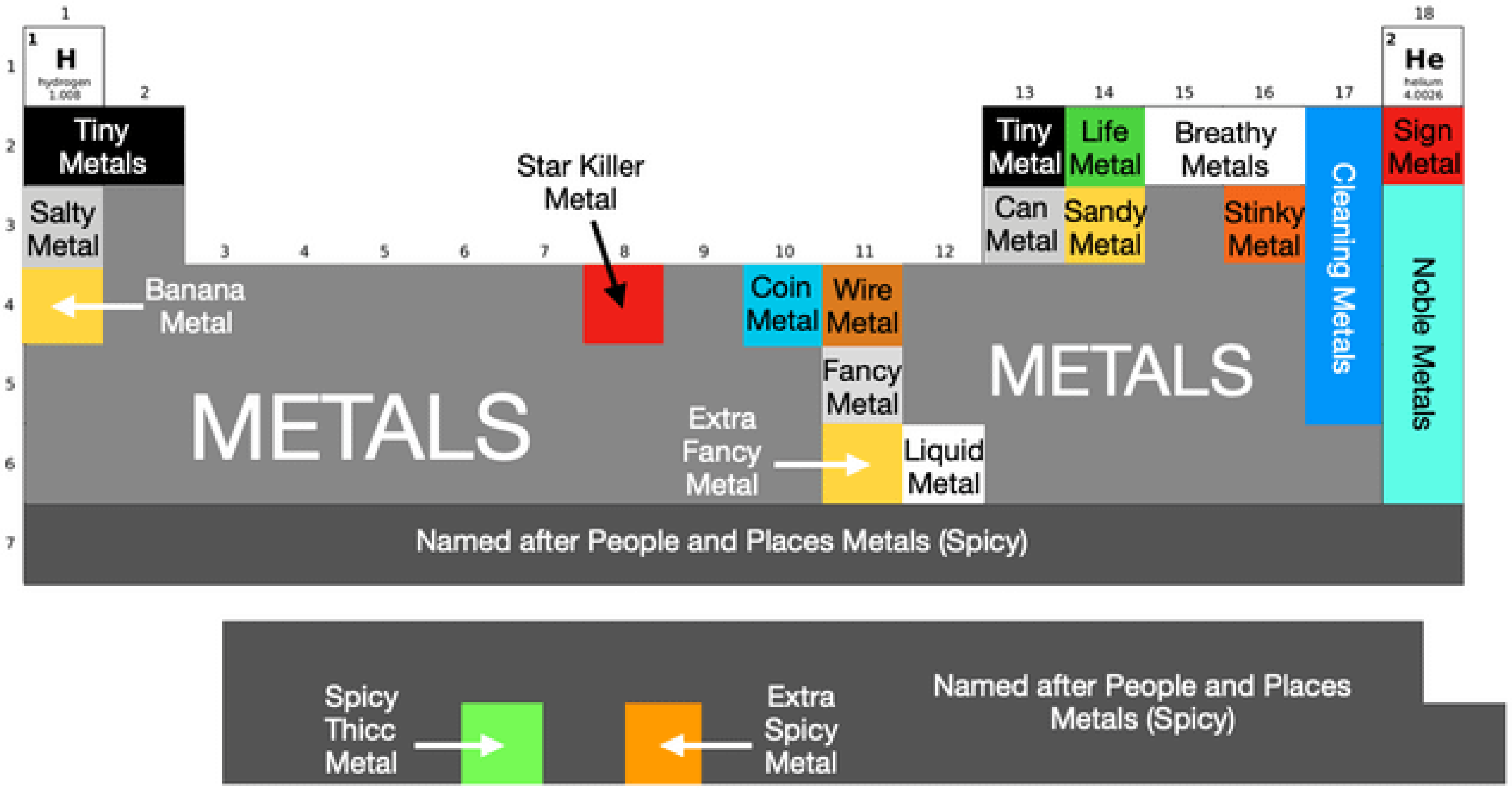
1
H
hydrogen
1.008
2
Tiny Metals
Salty Metal
Banana Metal
METALS
Star Killer Metal
3
4
5
6
7
8
9
10
11
12
Coin Metal
Wire Metal
Fancy Metal
Extra Fancy Metal
Liquid Metal
13
14
15
16
17
18
He
helium
4.0026
Tiny Metal
Life Metal
Breathy Metals
Can Metal
Sandy Metal
Stinky Metal
Cleaning Metals
Sign Metal
Noble Metals
METALS
Named after People and Places Metals (Spicy)
Spicy Thicc Metal
Extra Spicy Metal
Named after People and Places Metals (Spicy)

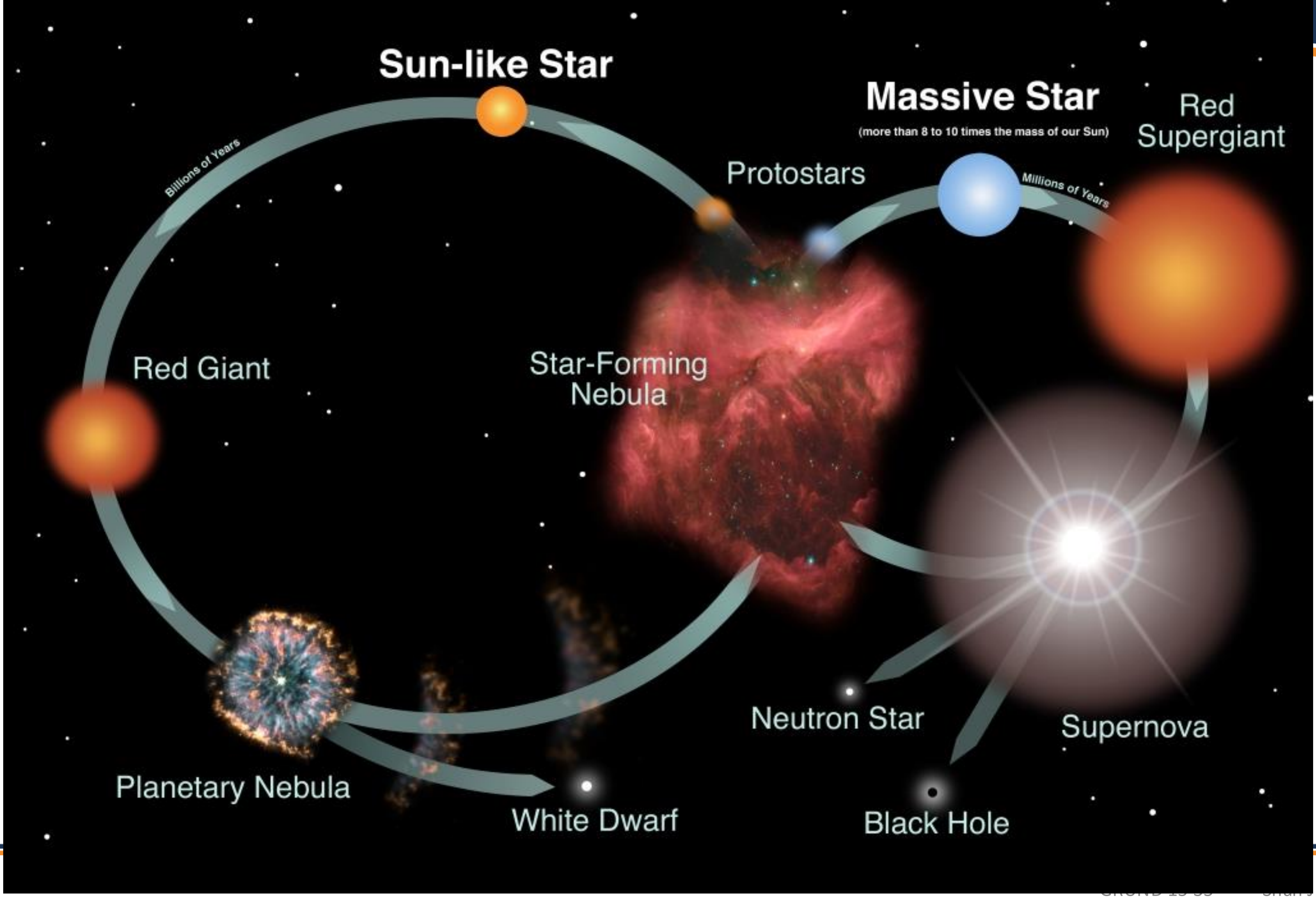
Sun-like Star
Billions of Years
Massive Star
(more than 8 to 10 times the mass of our Sun)
Red Supergiant
Protostars
Millions of Years
Red Giant
Star-Forming Nebula
Neutron Star
Supernova
Planetary Nebula
White Dwarf
Black Hole

NASA

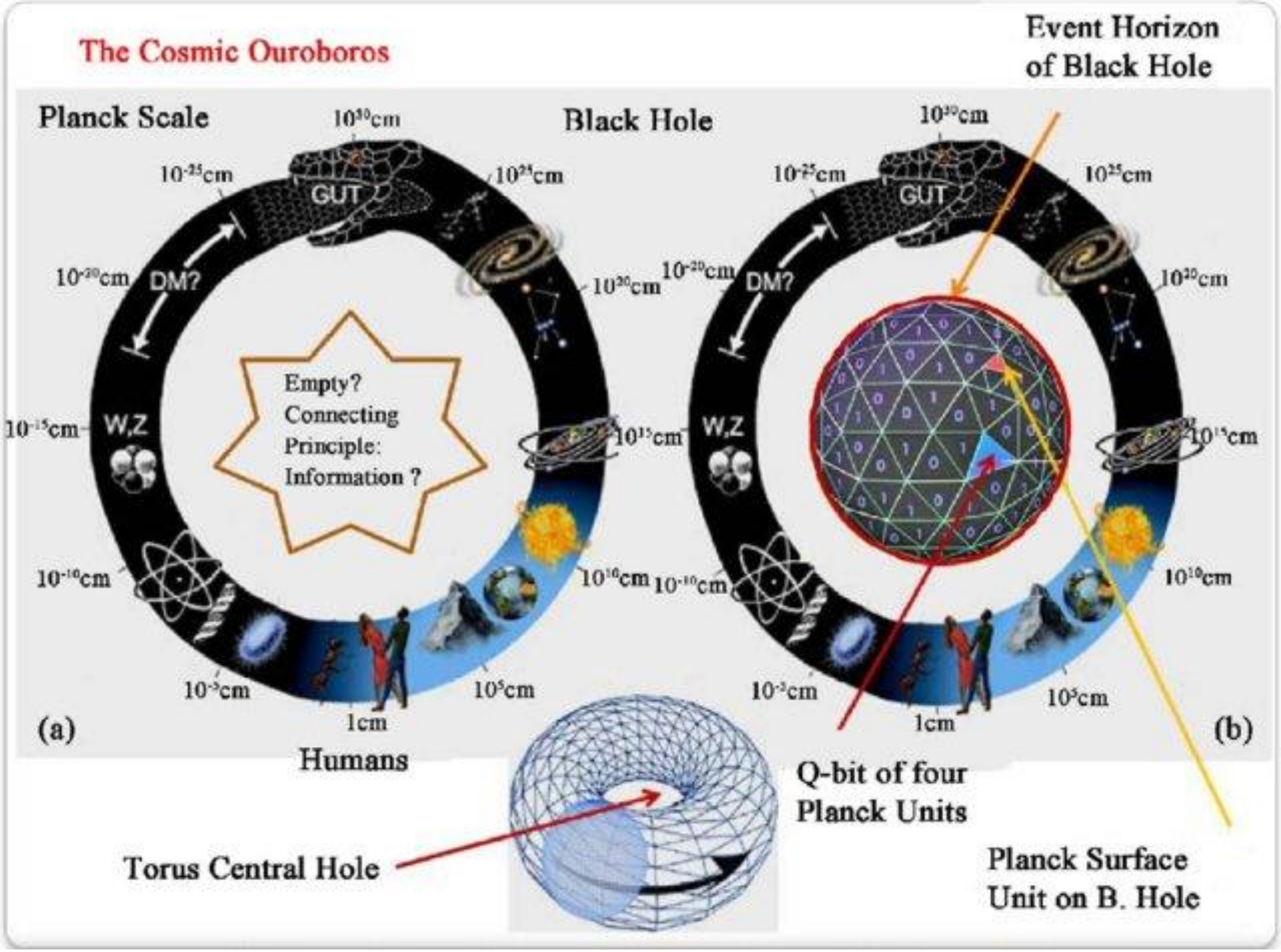
The Cosmic Ouroboros
Event Horizon of Black Hole
Planck Scale
Black Hole
GUT
DM?
W,Z
Empty? Connecting Principle: Information ?
Humans
(a)
(b)
Torus Central Hole
Q-bit of four Planck Units
Planck Surface Unit on B. Hole
1cm

Constituent of interstellar space	Where found	Temperature (K) Density (atoms/cm^3)	How best observed
Atomic Hydrogen (HI)	Everywhere (~50% of mass, ~50% of volume)	100 - 10^4 K 1 - 100 cm^{-3}	21-cm radio line Ultraviolet absorption lines
Molecular Hydrogen (H_2)	Dark clouds (~50% of mass, ~1% of volume)	5 - 100 K 10^4 - 100 cm^{-3}	Ultraviolet absorption lines Infrared emission lines
Other Molecules (e.g., CO, HCN, H_2O, etc.)	Dark Clouds	5 - 100 K 10^6 - 100 cm^{-3}	Radio and infrared emission lines
Ionized Hydrogen (HII)	Near hot stars (Emission nebulae)	5000 K 10^2 - 10^4 cm^{-3}	Optical and infrared emission lines; radio continuum
Coronal Gas	Everywhere (~50% of volume)	10^6 - 10^7 K 10^{-2} cm^{-3}	X-ray emission
Dust grains	Everywhere	20 - 100 K	Reddening and absorption of starlight; Infrared emission
Magnetic Fields	Everywhere		Polarization of starlight; Zeeman effect
Cosmic Rays	Everywhere		Radio emission, gamma ray emission

TABLE 1.1: Size-sorted molecules detected in the interstellar medium and in circumstellar shells, up to the year 2019. [8]

2 atoms	**3 atoms**	**4 atoms**	**5 atoms**	**6 atoms**	**7 atoms**	**8 atoms**
H_2	C_3	c-C_3H	C_5	C_5H	C_6H	CH_3C_3N
AlF	C_2H	l-C_3H	C_4H	l-H_2C_4	CH_2CHCN	$HC(O)OCH_3$
AlCl	C_2O	C_3N	C_4Si	C_2H_4	CH_3C_2H	CH_3COOH
C_2	C_2S	C_3O	l-C_3H_2	CH_3CN	HC_5N	C_7H
CH	CH_2	C_3S	c-C_3H_2	CH_3NC	CH_3CHO	C_6H_2
CH^+	HCN	C_2H_2	H_2CCN	CH_3OH	CH_3NH_2	CH_2OHCHO
CN	HCO	NH_3	CH_4	CH_3SH	c-C_2H_4O	l-HC_6H
CO	HCO^+	HCCN	HC_3N	HC_3NH^+	H_2CCHOH	CH_2CHCHO
CO^+	HCS^+	$HCNH^+$	HC_2NC	HC_2CHO	C_6H^-	CH_2CCHCN
CP	HOC^+	HNCO	HCOOH	NH_2CHO	CH_3NCO	H_2NCH_2CN
SiC	H_2O	HNCS	H_2CNH	C_5N	HC_5O	CH_3CHNH
HCl	H_2S	$HOCO^+$	H_2C_2O	l-HC_4H	$HOCH_2CN$	CH_3SiH_3
KCl	HNC	H_2CO	H_2NCN	l-HC_4N		$H_2NC(O)NH_2$
NH	HNO	H_2CN	HNC_3	c-H_2C_3O		
NO	MgCN	H_2CS	SiH	H_2CCNH		
NS	MgNC	H_3O^+	H_2COH^+	C_5N^-		
NaCl	N_2H^+	c-SiC_3	C_4H^-	HNCHCN		
OH	N_2O	CH_3	HC(O)CN	SiH_3CN		
PN	NaCN	C_3N^-	HNCNH	C_5S		
SO	OCS	PH_3	CH_3O	MgC_4H		
SO^+	SO_2	HCNO	$NH_4{}^+$			
SiN	c-SiC_2	HOCN	H_2NCO^+			
SiO	CO_2	HSCN	$NCCNH^+$			
SiS	NH_2	H_2O_2	CH_3Cl			
CS	$H_3{}^+$	C_3H^+	MgC_3N			
HF	SiCN	HMgNC				
HD	AlNC	HCCO				
FeO	SiNC	CNCN				
O_2	HCP	HONO				
CF^+	CCP	MgC_2H				
SiH	AlOH					
PO	H_2O^+	**9 atoms**	**10 atoms**	**11 atoms**	**12 atoms**	**>13 atoms**
AlO	H_2Cl^+	CH_3C_4H	CH_3C_5N	HC_9N	c-C_6H_6	C_{60}
OH^+	KCN	CH_3CH_2CN	$(CH_3)_2CO$	CH_3C_6H	n-C_3H_7CN	C_{70}
CN^-	FeCN	$(CH_3)_2O$	$(CH_2OH)_2$	C_2H_5OCHO	i-C_3H_7CN	$C_{60}{}^+$
SH^+	HO_2	CH_3CH_2OH	CH_3CH_2CHO	$CH_3OC(O)CH_3$	$C_2H_5OCH_3$	c-C_6H_5CN
SH	TiO_2	HC_7N	CH_3CHCH_2O			
HCl^+	C_2N	C_8H	CH_3OCH_2OH			
TiO	Si_2C	$CH_3C(O)NH_2$				
ArH^+	HS_2	C_8H^-				
N_2	HCS	C_3H_6				
NO^+	HSC	CH_3CH_2SH				
NS^+	NCO	CH_3NHCHO				
HeH^+	CaNC	HC_7O				

TABLE 2

Chemical Composition of Different Object Classes in the Solar Neighborhood and of the Sun

Elem.	Cosmic Standard B Stars–This Work[a]		Orion Gas+Dust[b]	B Stars[c]	Young F&G Stars[c]	ISM		Sun	
						Gas	Dust[d]	GS98[e]	AGS05[e]
He	10.98 ± 0.02	...	10.988 ± 0.003	...	...	...	...	10.99 ± 0.02	
C	8.32 ± 0.03	209 ± 15	8.52 ± 0.02	8.28 ± 0.17	8.55 ± 0.10	8.15 ± 0.06[f]	68 ± 26	8.52 ± 0.06	8.39 ± 0.05
N	7.76 ± 0.05	58 ± 7	7.73 ± 0.09	7.81 ± 0.21	...	7.79 ± 0.03[g]	...	7.92 ± 0.06	7.78 ± 0.06
O	8.76 ± 0.03	575 ± 41	8.73 ± 0.03	8.54 ± 0.16	8.65 ± 0.15	8.59 ± 0.01[h]	186 ± 42	8.83 ± 0.06	8.66 ± 0.05
Ne	8.08 ± 0.03	120 ± 9	8.05 ± 0.07	...	...	...	...	8.08 ± 0.06	7.84 ± 0.06
Mg	7.56 ± 0.05	36 ± 4	...	7.36 ± 0.13	7.63 ± 0.17	6.17 ± 0.02[i]	34.8 ± 4.4	7.58 ± 0.05	7.53 ± 0.09
Si	7.50 ± 0.02	32 ± 1	...	7.27 ± 0.20	7.60 ± 0.14	6.35 ± 0.05[i]	29.6 ± 2.2	7.55 ± 0.05	7.51 ± 0.04
Fe	7.44 ± 0.04	28 ± 3	...	7.45 ± 0.26	7.45 ± 0.12	5.41 ± 0.04[i]	27.3 ± 2.7	7.50 ± 0.05	7.45 ± 0.05

Notes.—(a) In units of log(El/H) + 12 / atoms per 10^6 nuclei, computed from average star abundances (mean values over all individual lines *per element*, equal weights per line); (b) Esteban et al. (2004); (c) Sofia & Meyer (2001); (d) difference between the cosmic standard and ISM gas-phase abundances, in units of atoms per 10^6 H nuclei; (e) photospheric values; (f) Sofia (2004); (g) Meyer et al. (1997), corrected accordingly to Jensen et al. (2007); (h) Cartledge et al. (2004); (i) Cartledge et al. (2006).

$FeH^+Ar_{1,2}$: UV-Vis Spectrum

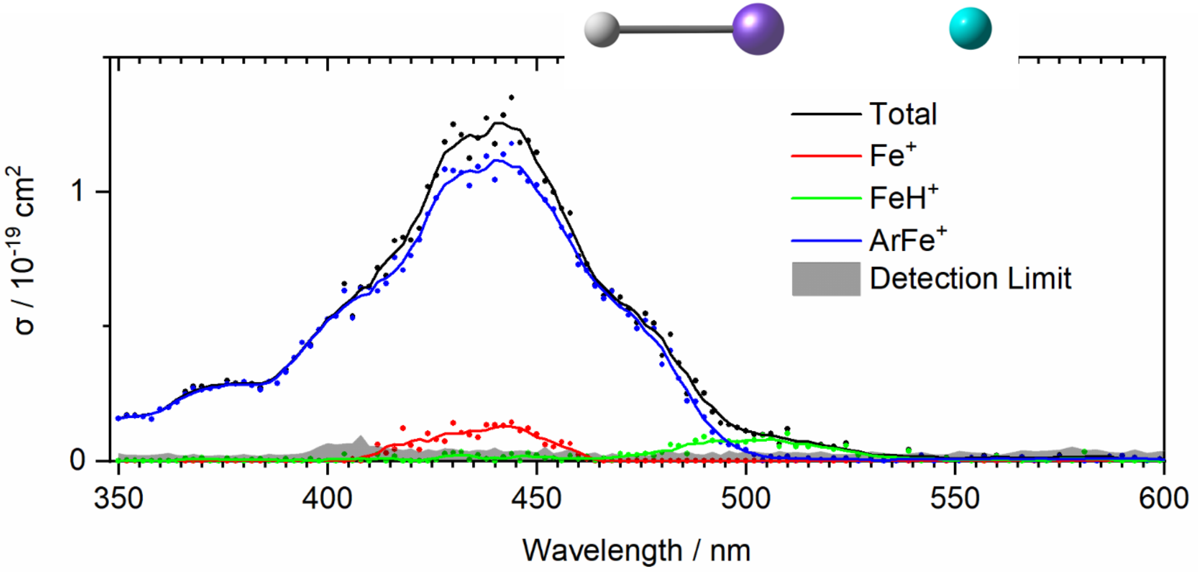

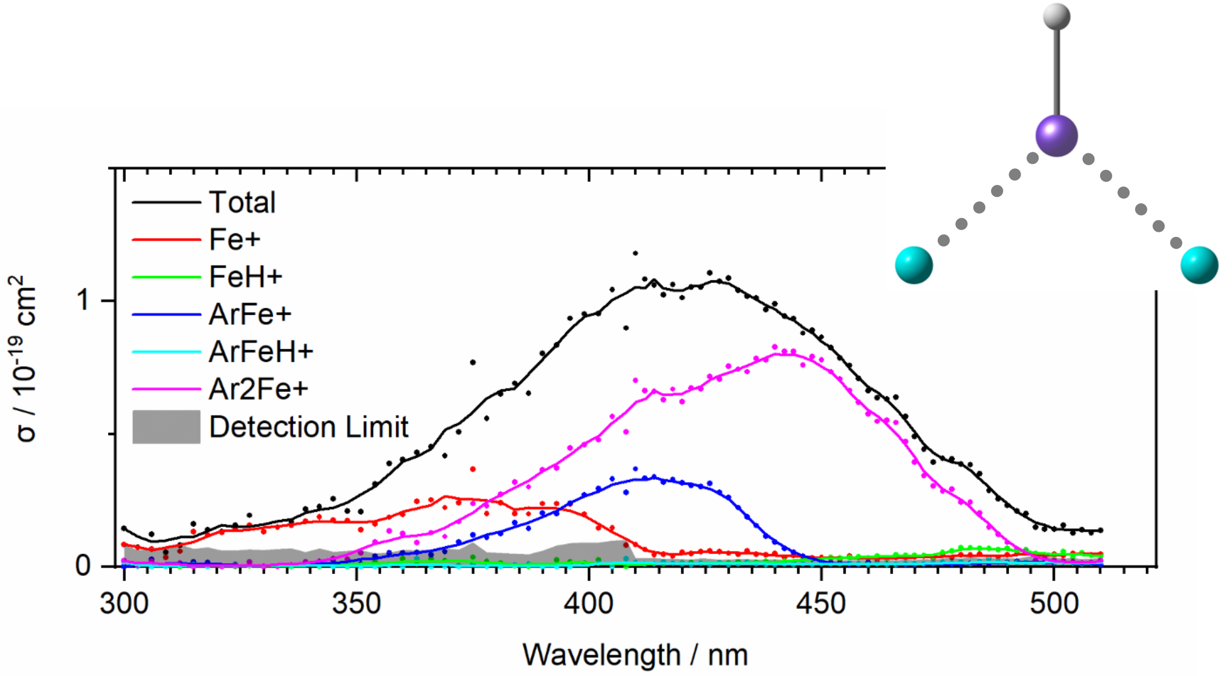

reactants	products	Dissociation energy[a] /eV	Dissociation energy[b] /eV
$ArFeH^+$ + hν	$ArFe^+$ + H·	2.45	2.76
	FeH^+ + Ar	0.46	0.5
	Fe^+ + Ar + H·	2.61	3.03
Ar_2FeH^+ + hν	$Ar2Fe^+$ + H·	2.62	2.9
	$ArFe^+$ + Ar + H·	2.75	3.11
	$ArFeH^+$ + Ar	0.3	0.35
	FeH^+ + 2Ar	0.76	0.85
	Fe^+ + 2Ar + H·	2.91	3.38